Numerical Simulation of A Complicated Transition-Breakdown of Vortical Flows inside a Circular Pipe

By

H.L.CHEN* AND K. OSHIMA**

(May 1, 1990)

Abstract: Entrance flows to a circular pipe which has an axisymmetric sudden expansion were numerically simulated for a wide range of Reynolds numbers. Particularly shear layer instabilities observed behind the sudden expansion were studied. Experimental observation of the flow fields at the corresponding flow conditions were also carried out. Taylor-Helmholtz type instability was observed along the shear layer behind the sudden expansion, and its breakdown into turbulent blobs were observed. Numerical results successfully simulated this vortex breakdown process. The process that flows grow into chaos were also successfully simulated.

1. INTRODUCTION

With recent high performance computers and advanced numerical methods, it has become possible to solve the detailed dynamical behaviors of the time-dependent Navier-Stokes equations. This becomes a new, important way to study the transition and other complicate physical phenomena. In this study, We use numerical simulation method to study stability problems of circular pipe flow. The flow inside a pipe of circular cross-section is one of the most classic, yet important problems because it includes fundamental mechanism of flow instability and turbulence transition. On the numerical simulation aspect, H. Kanda and K. Oshima [6] have completed the numerical simulation of impulsively started axisymmetric circular pipe flow. Their simulation results show that, regardless of the flow Reynolds number based on the mean velocity and the pipe diameter, the velocity distribution tends to the Poiseuille type, after start from rest condition. That is, this type of flow is stable, which agree with the prediction derived from the linear stability analysis [8]. When axisymmetric disturbance is superposed to the uniform entrance flow, the disturbance grows and eventually yields reverse flow regions. This suggests turbulence transition, which agree with nonlinear stability analysis [11]. In present work, We study the detailed vortex breakdown process and investigate the evolution and the structure of vortical flow at unsteady flow regime. Replacing the artificial disturbance at the inlet, axisymmetric sudden expansion geometries of various size are set. It is assumed that fluid flow impulsively started from rest condition. At low Reynolds numbers, flows are steady one, with a finite lengh reverse zone. Many experimental and numerical research have been carried out in this regime [4]. Numerical simulation was successful. However, as the Reynolds number increasing, flow become unsteady and the reattachment point disappear. Evolution of the shear layer behind the sudden expansion, together with

* Department of Aeronautical Engineering, University of Tokyo
** The Institute of Space and Astronautical Science 3-1-1 Yoshinodai, Sagamihara 229, Japan

This document is provided by JAXA.

its interaction with the boundary layer on the wall of the pipe, causes complicated transition-breakdown of vortical flow. Flows in this regime are not elucidated yet. In order to simulate complicated flows under various conditions, we developed an efficient calculation code. Experimental observation of flow field at corresponding flow conditions are also carried out. In the following section, We will describe the numerical method briefly and discuss the numerical and experimental results.

2. Numerical Method

In this simulation, fluid flow is assumed to be incompressible, axisymmetric. Independent variables are Stokes stream-function ϕ, vorticity ω and swirling velocity W. The Stokes stream function defined as:

$$U=-\frac{1}{r}\frac{1\partial\phi}{\partial r},\quad V=\frac{1}{r}\frac{1\partial\phi}{r\partial z} \tag{1}$$

Here the U, V, W is the axial, radial velocity or swirling velocity in (z, r, θ) plane. The circumferential component of vorticity is:

$$\omega=\frac{\partial U}{\partial r}-\frac{\partial V}{\partial z} \tag{2}$$

Driven from mass conversation equation, the relation between stream function and vorticity is

$$\frac{1}{r}\left(\frac{\partial^2\phi}{\partial z^2}+\frac{\partial^2\phi}{\partial r^2}\right)-\frac{1}{r^2}\frac{\partial\phi}{\partial r}=-\omega \tag{3}$$

The vorticity transport equation in non-conservative form is:

$$\frac{\partial\omega}{\partial t}+U\frac{\partial\omega}{\partial z}+V\frac{\partial\omega}{\partial r}-V\frac{\omega}{r}=-\frac{1}{r}\frac{\partial W^2}{\partial r}\frac{1}{Re}\left(\frac{\partial^2\omega}{\partial r^2}+\frac{\partial^2\omega}{\partial r^2}+\frac{\partial\omega}{r\partial r}-\frac{\omega}{r^2}\right) \tag{4}$$

The momentum equation at θ direction in non-conservative form is:

$$\frac{\partial W}{\partial t}+U\frac{\partial W}{\partial z}+V\frac{\partial W}{\partial r}+V\frac{W}{r}=\frac{1}{Re}\left(\frac{\partial^2 W}{\partial z^2}+\frac{\partial^2 W}{\partial r^2}+\frac{\partial W}{r\partial r}-\frac{W}{r^2}\right) \tag{5}$$

Here the Re is the Reynolds number, which based on the mean velocity and the diameter of the pipe.

The finite difference method are applied to obtain numerical solution of above equations. In order to simulate flow at high Reynolds number, numerical scheme is require to have good stability. Therefore, two-second order upwind scheme is applied in convection terms, alternative direction implicit difference is applied in time derivative, diffusion terms are two-order central difference. Detail description of the numerical scheme are summarized in the report [7].

Non-slip and continuum conditions are fulfilled on the wall of the pipe. Entrance flow is uniform in this simulation. Axisymmetric conditions are given on the axis. The values of the stream function, the vorticity and the swirling velocity on the exit are extrapolated.

This document is provided by JAXA.

Stability of the scheme is based on a empirical consideration. That is, in each time step, the moved distance of fluid particle is shorter than one grid space. The grid space is given by geometry and number of grid, then the time step is given in above way.

Two mesh system are used in the simulation. Fine mesh system is 601*31, coarse one is the 301*16. Length of the pipe is twenty time of the diameter of the pipe. Simulation of unsteady flow requires large calculation length and small time step. Considering that fluid particle on the axis passes through whole length of pipe in about 15 (non-dimensionalized time), total calculation length is set as 75 (nondimensionalized time). The number of time step is 7500. This length is thought to be enough to catch the change of flow field after starting vortex passed.

Numerical simulations were carried out over from 100 to 100000 of the Reynolds numbers. The CPU time and the memory for typical case in numerical simulation are listed in Tab. 1. In the pipe flow, geometry characteristics is that dimension in the axial direction is very long. Therefore the large numbers of grids are require in this direction. Rectangular grid, $\Delta z = n\Delta r$, may reduce the grid number in axial direction. But at a large n, the stability of scheme becomes bad. In above simulation, the n is select as 2. Comparing with related experiment, in which the pipe diameter is 3 cm and the fluid is water, the minimum vortex blob and the maximum wave number that can be recognized in grid system B are about 2 mm, 1 kHz, respectively. To simulate smaller size vortex which has the order of real turbulence flow, ideal one is grid system C. it is predicted that about 30 hours CPU time is require in grid system C. If to simulation three-dimensional flow, several ten time of CPU time and memory will be necessary. For example, Calculation of three-dimensional flow at level of grid system B may take as much CPU time as about 40 hours.

	CPU time of M780	CPU time of VP200	Memory
Grid system A 301 × 16	95 min.	11 min.	1.8 Mbyte
Grid system B 601 × 31	*600 min.	65 min.	2.6 Mbyte
Grid system C 2001 × 101	——	*1800 min.	*15 Mbyte

Table 1. The CPU time and memory of the simulation. The calculation length is 75 nondimensional time. FACOM M-780 are the main frame computer of ISAS. FACOM VP-200 is the supercomputer of ISAS, its calculation capacity is 500 MFLOPS. The * is predicted values.

3. Results and Discussions

3.1 Taylor-Helmholtz type instability and vortex breakdown

Numerical results show that After impulsively started from rest, flow tends to steady state at low Reynolds numbers. Laminar, recirculation vortex region forms and velocity distribution is Poiseuille type in downstream. Flow pattern in such case are shown in Fig. 1. As Reynolds number increase, reattachment point disappears and flow is unsteady. Vortex rings shed along the shear layer, as shown in Fig. 2. The flow pattern

This document is provided by JAXA.

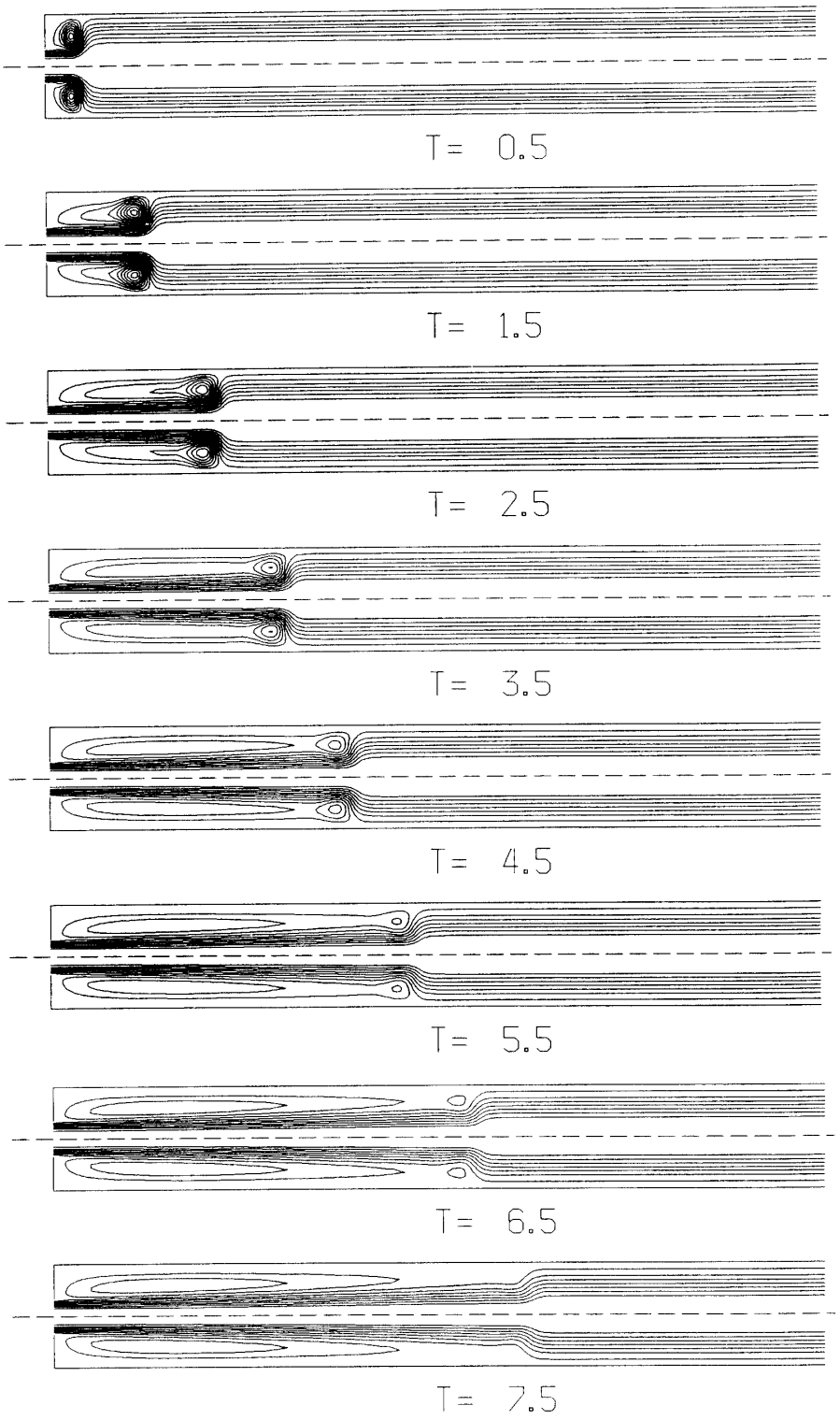

Fig. 1. Flow patterns after impulsively started from the rest condition, the Reynolds number is 100.

This document is provided by JAXA.

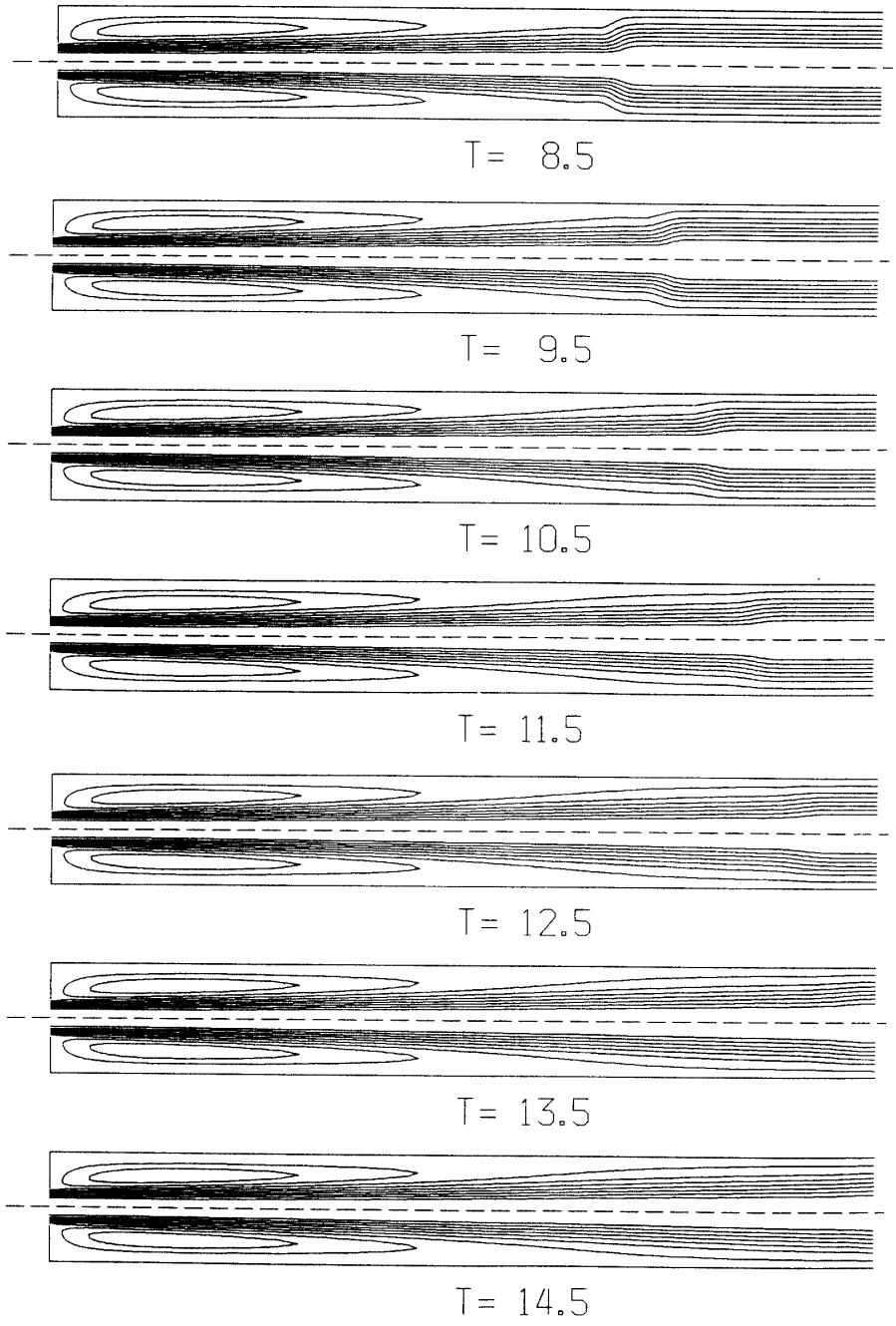

Fig. 1 (Continued)

This document is provided by JAXA.

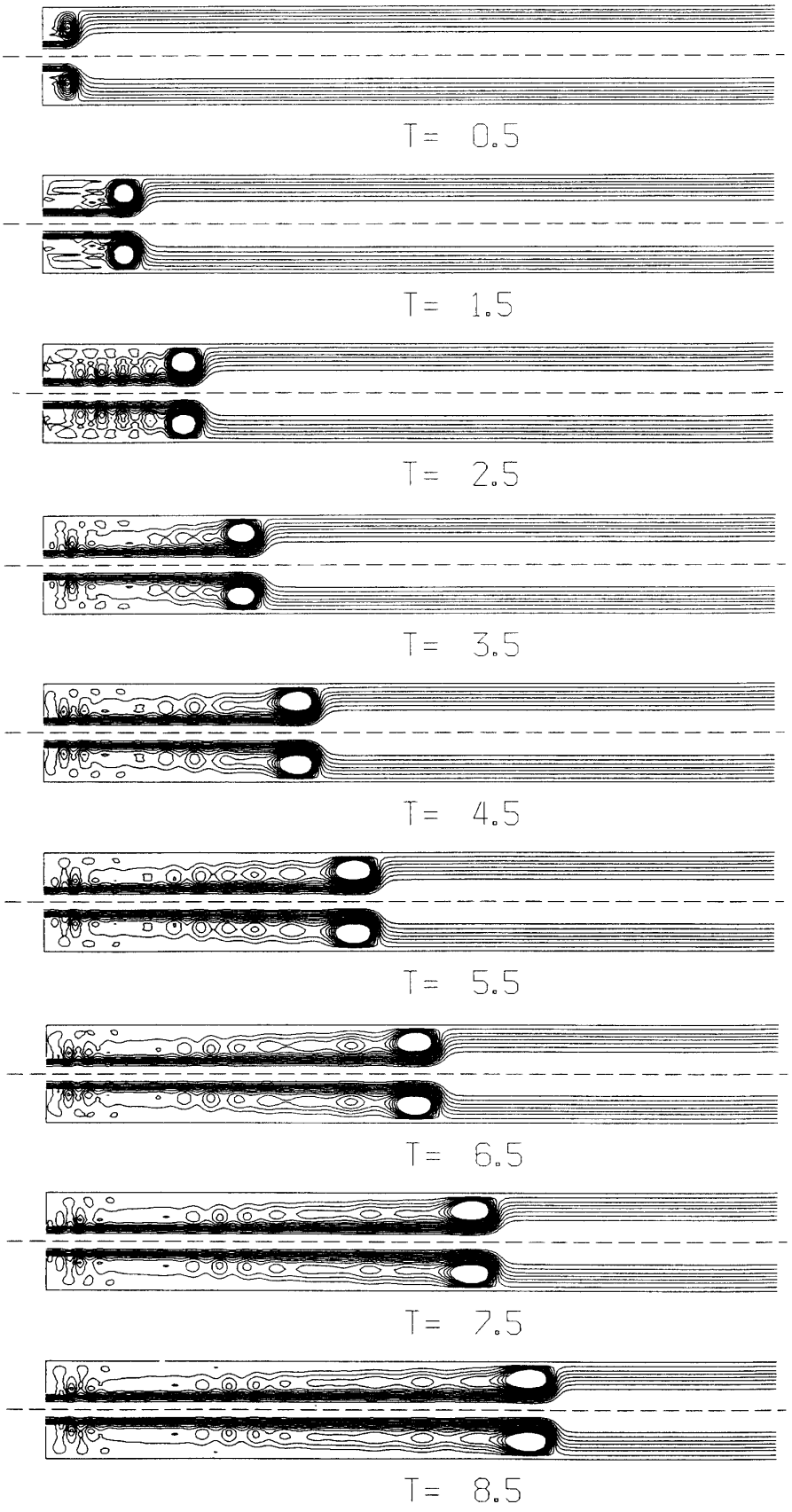

Fig. 2. Flow patterns after impulsively started from the rest condition, the Reynolds number is 2000.

This document is provided by JAXA.

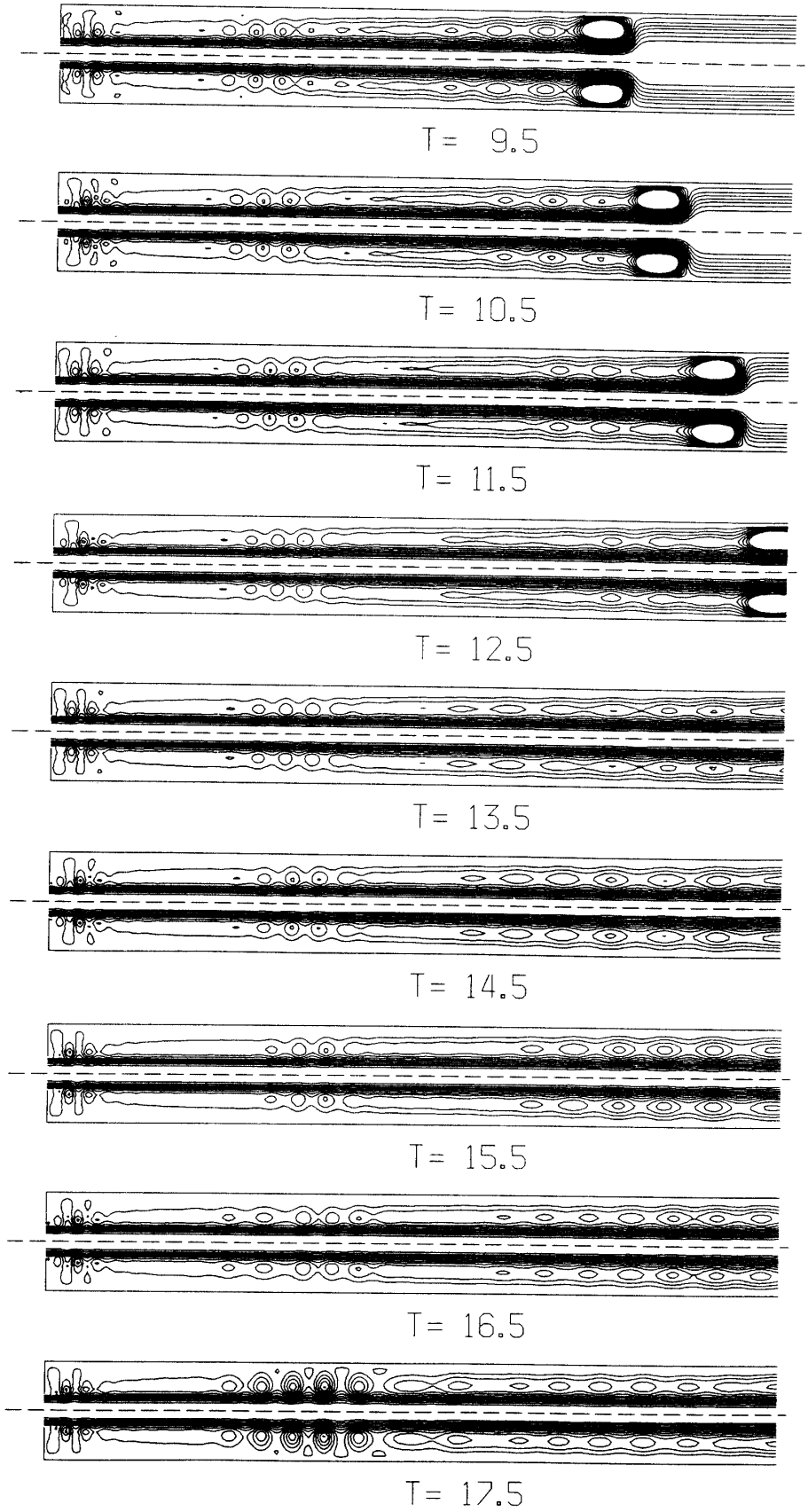

Fig. 2 (Continued)

This document is provided by JAXA.

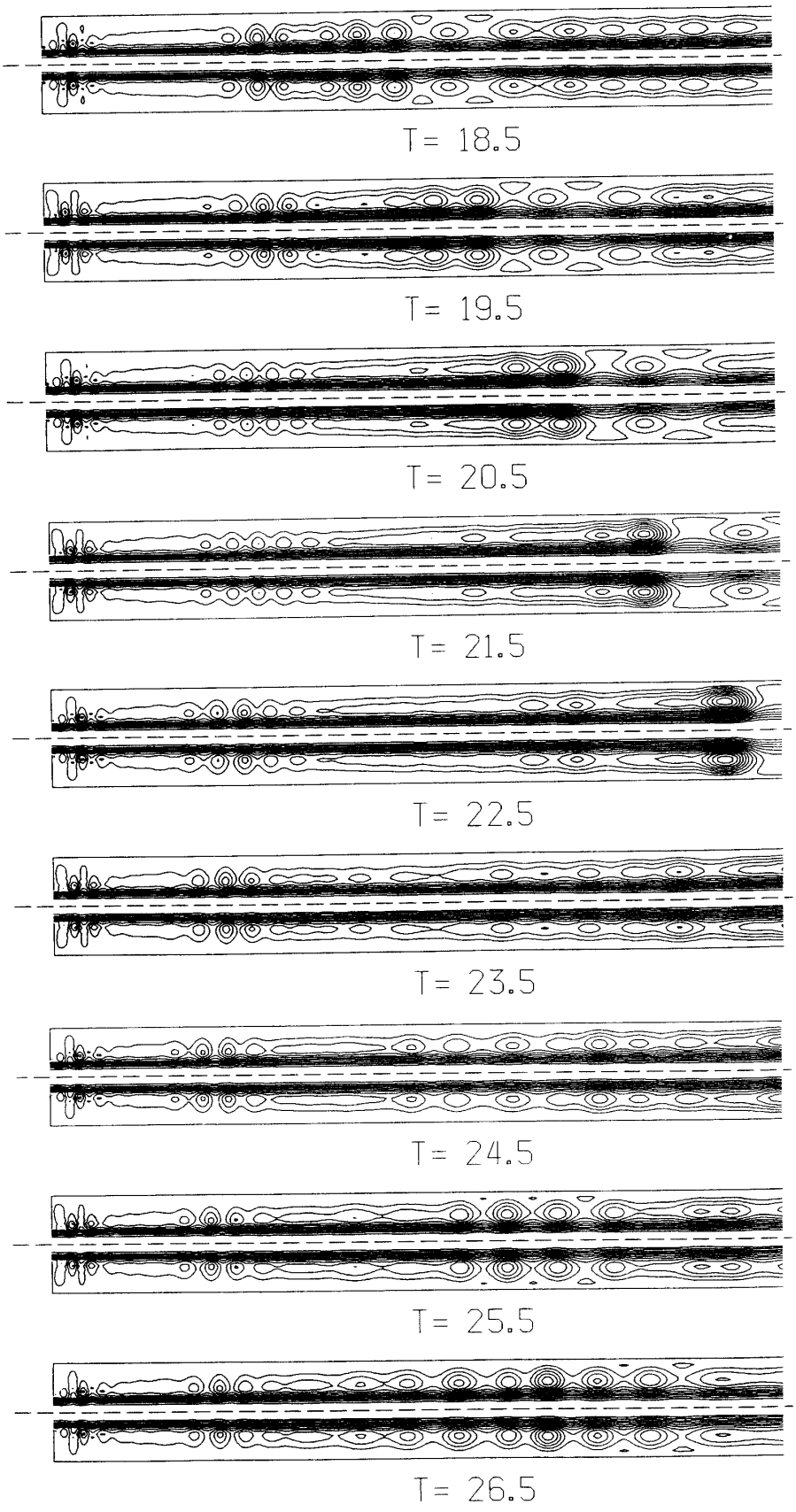

Fig. 2 (Continued)

This document is provided by JAXA.

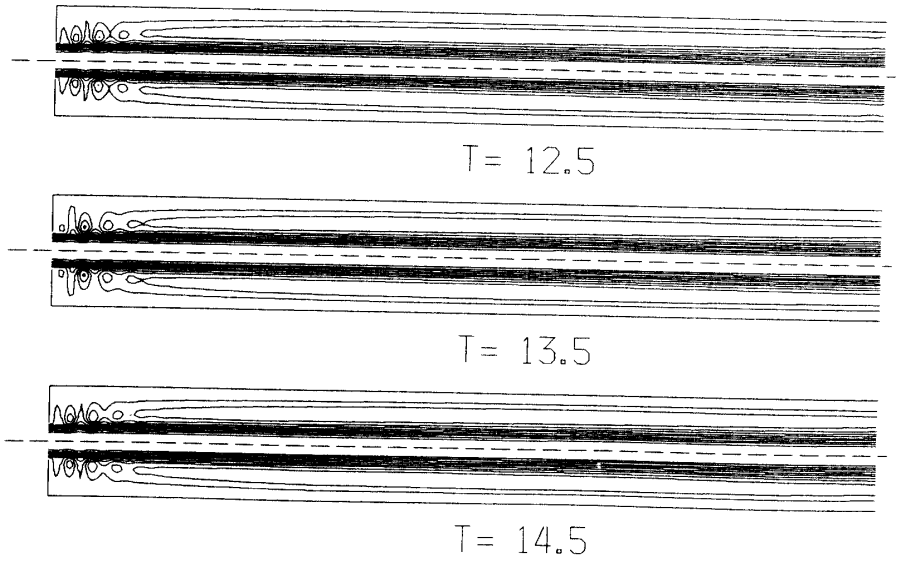

Fig. 3. Flow patterns at Re=500.

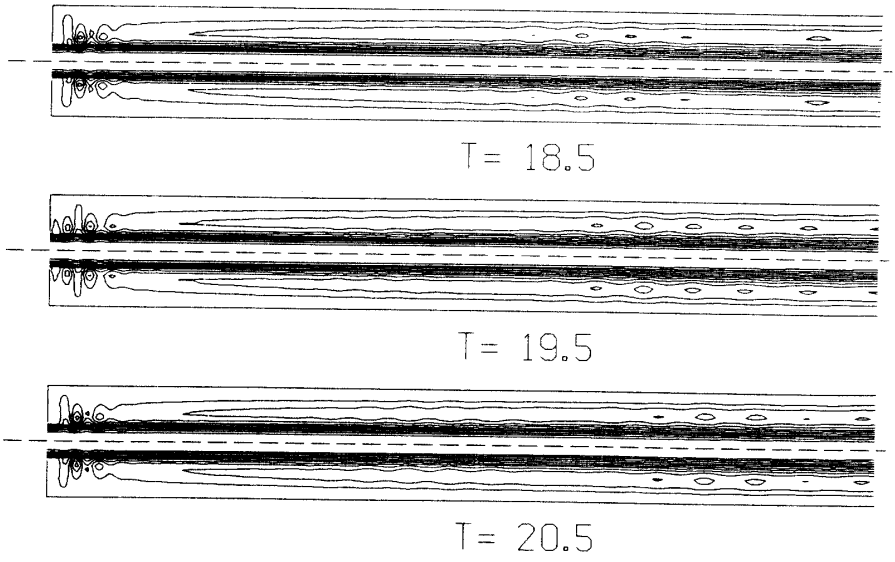

Fig. 4. Flow patterns at Re=1000.

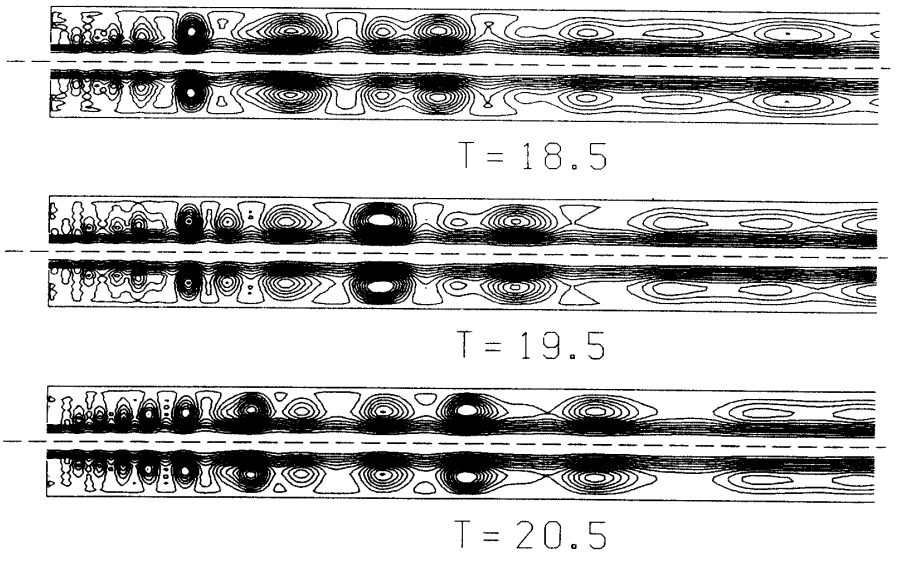

Fig. 5. Flow patterns at Re=10000.

This document is provided by JAXA.

at various Reynolds number are shown in Fig. 3, Fig. 4 and Fig. 5.

The shedding process of a street of vortices are successfully simulated. Vorticity distribution of around the shedding point at the Reynolds number 3000 are plotted it Fig. 6 In order to show the detailed vorticity distribution, the size at radial direction are enlarged. It can be seen that, before the shedding point, the equi-vorticity lines are parallel to the symmetric axis and the vorticity concentrates inside band region, which has a same mean radius as sudden expansion. It is a typical shear layer. Around the shedding point, the parallel vorticity distribution change sharply and shear layer suddenly burst into a number of vortex blobs of various size, the maximum vortcity appears in this point. The vorticity on the wall corresponding this point has a large

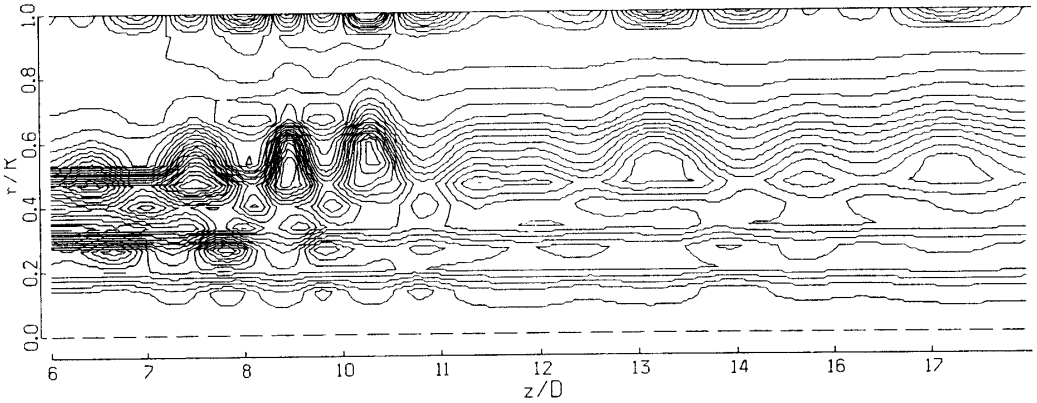

Fig. 6. Vorticity distribution at Re = 3000.

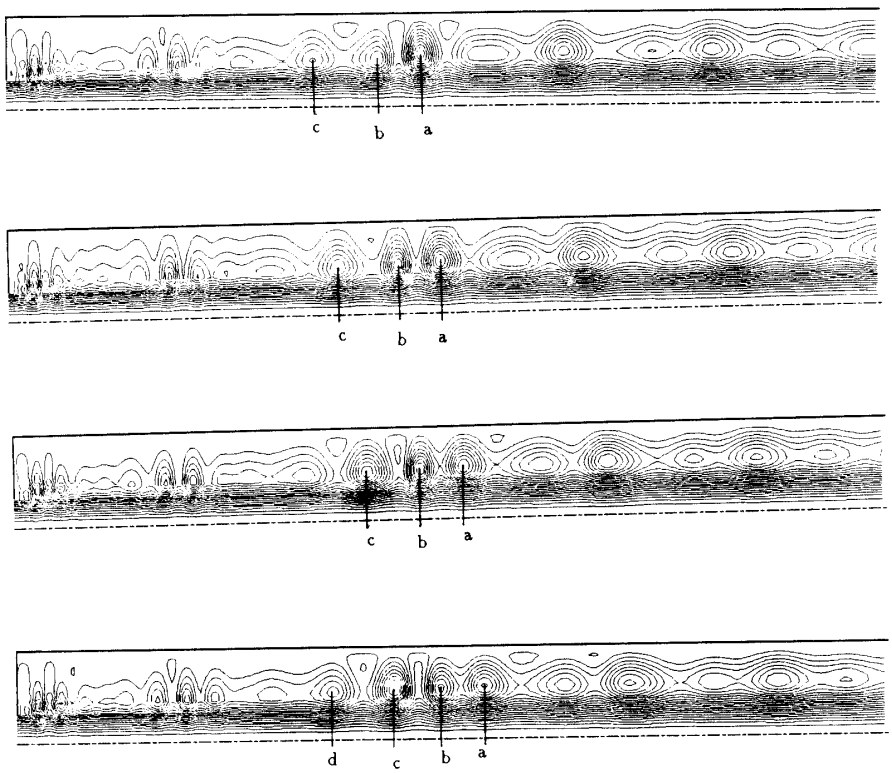

Fig. 7. The processes of vortex shedding and paring at Re = 3000.

This document is provided by JAXA.

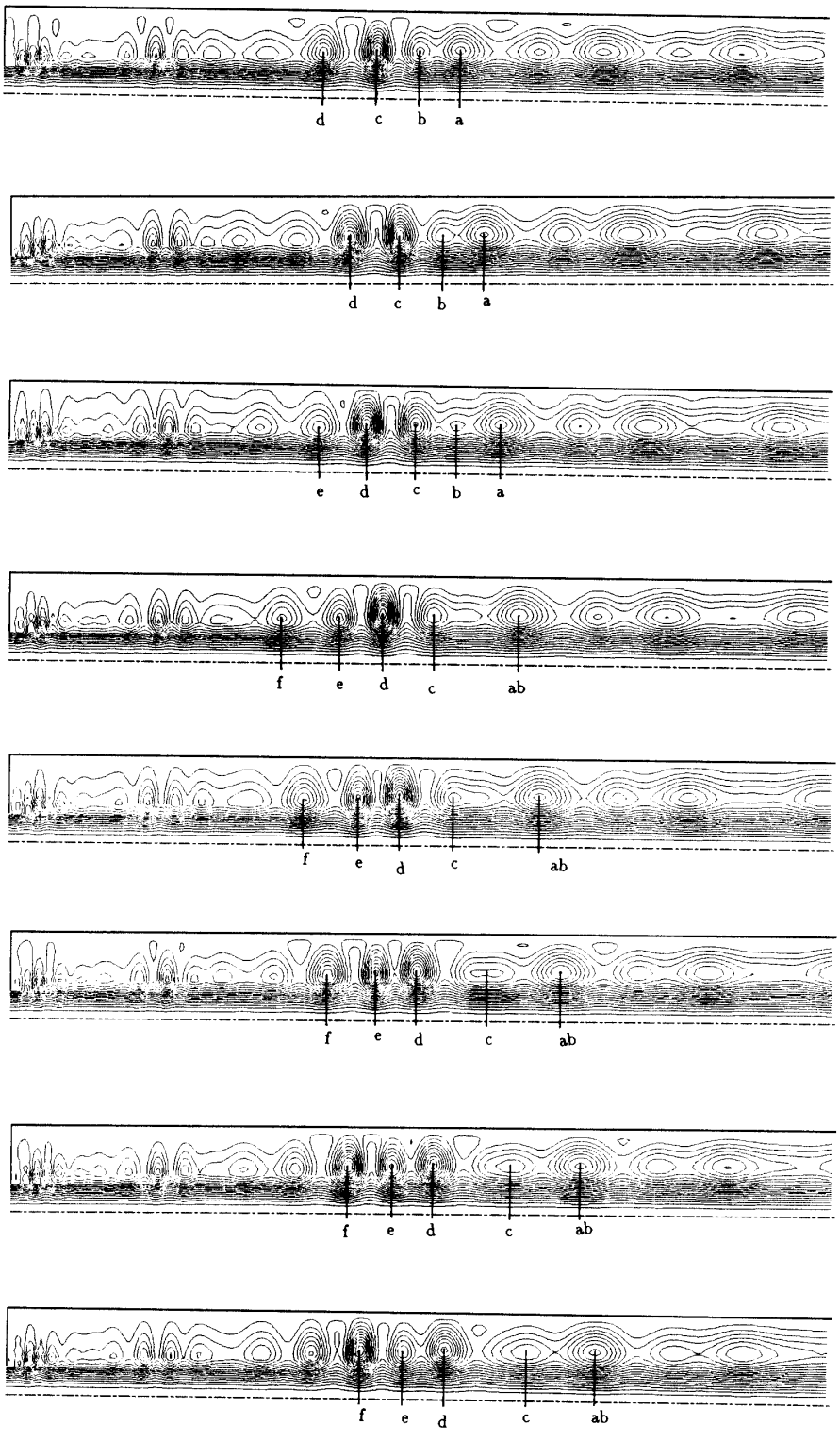

Fig. 7 (Continued)

This document is provided by JAXA.

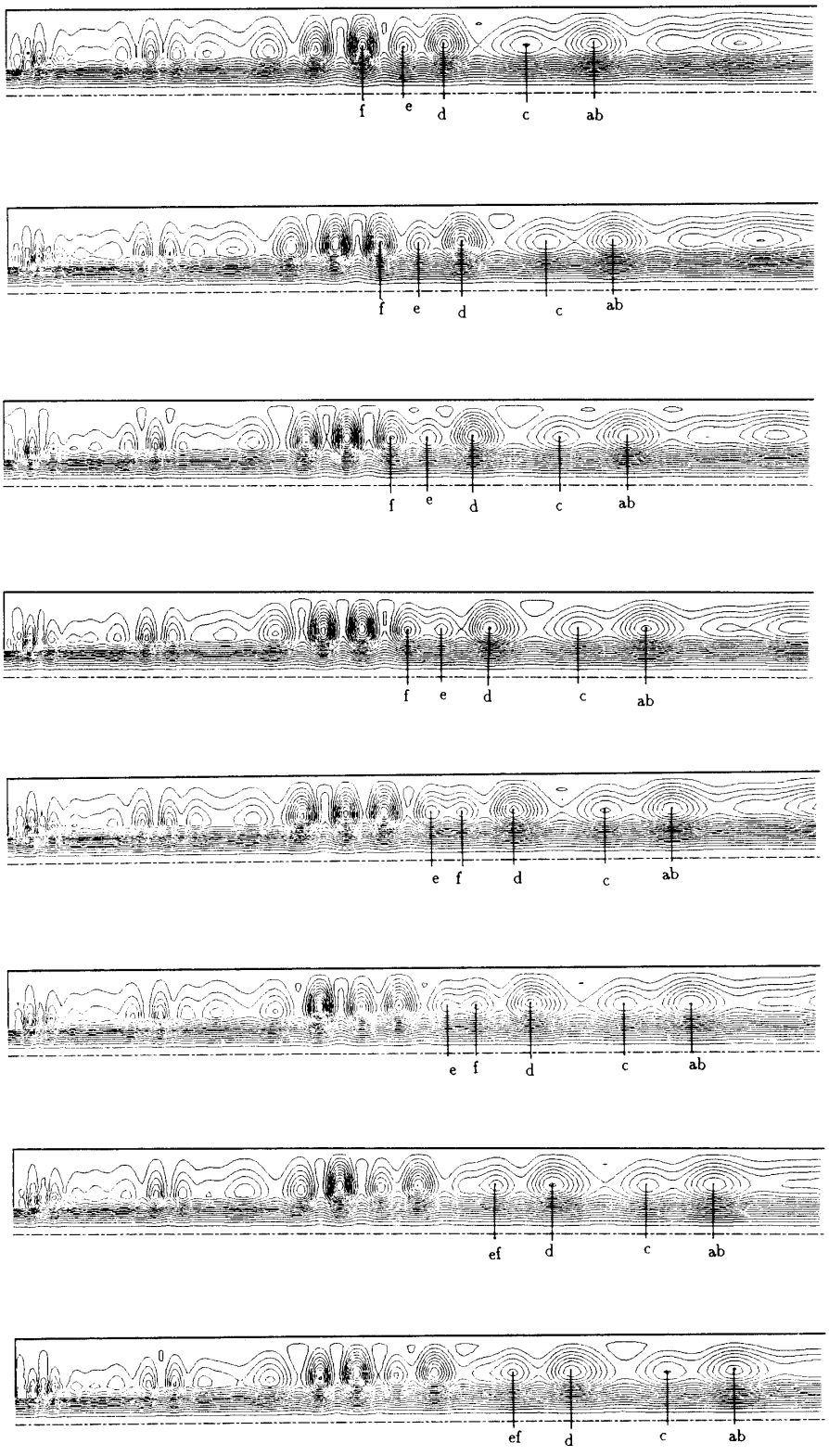

Fig. 7 (Continued)

This document is provided by JAXA.

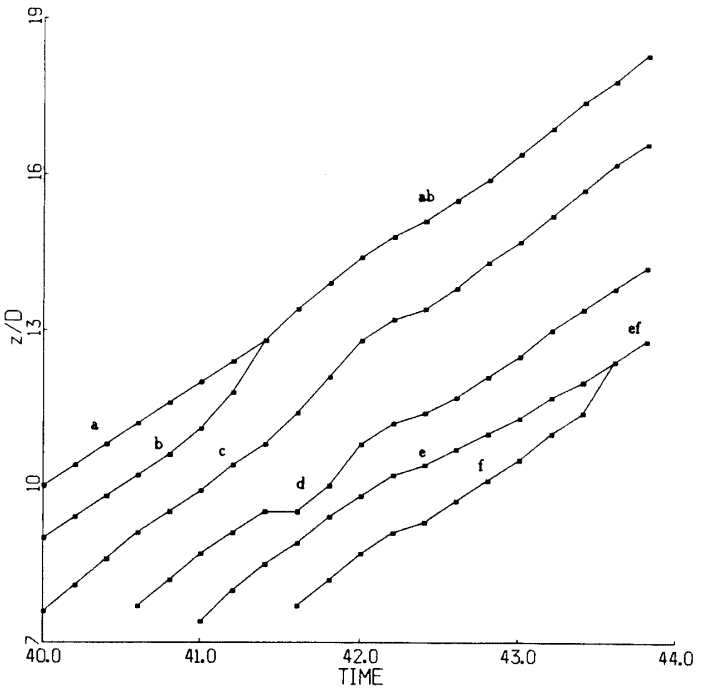

Fig. 8. Histry of vortices position by numerical simulation at Re=3000.

negative value. It is noted that the viscous effect and the boundary layer on the wall is also important in this stedding process. After the shedding point, the region of vorticity distribution extend. Complicated interaction of vortices are dominant in downstream, and chaotic behavior of flow appears. The corresponding stream lines at Reynolds number 3000 are plotted in Fig. 7.

Experimental results also confirm the Taylor-Helmholtz type instability and vortex breakdown process in circular-pipe flow which has an axisymmetric sudden expansion. The results of experimental observation are shown in Fig. 9 to Fig. 13. The same processes appear at lower Reynolds number in experimental observation. The absence of disturbance at inlet in numerical simulation may be the reason. The flow patterns in experimental observation at rarious Reynolds number are shown in Fig. 9. The position history of vortex rings are shown in Fig. 10. Transition distance at various sudden expansion ratio are plotted in Fig. 11. The Reynolds number dependence of Strouhal number from experimental observation as well as the numerical simulation are shown in Fig. 12 and Fig. 13.

The ratio of sudden expansion diameter and pipe diameter is 1/3 in above numerical results. The calculation and the experiment at different ratios were also carried out. At a large ratio, the same processes take place at higher Reynolds numbers. When the ratio is 1, that means the sudden expansion is removed, numerical results are completely agree with H. kanda and K. Oshima [6]. That is, regardless of the Reynolds number, velocity distribution tends to the Poiseuille type steady solution.

In above simulation, the swirling velocity was not considered. When swirling velocity is introduced at the inlet of pipe, the flow pattern is essentially different. Exceeding a

This document is provided by JAXA.

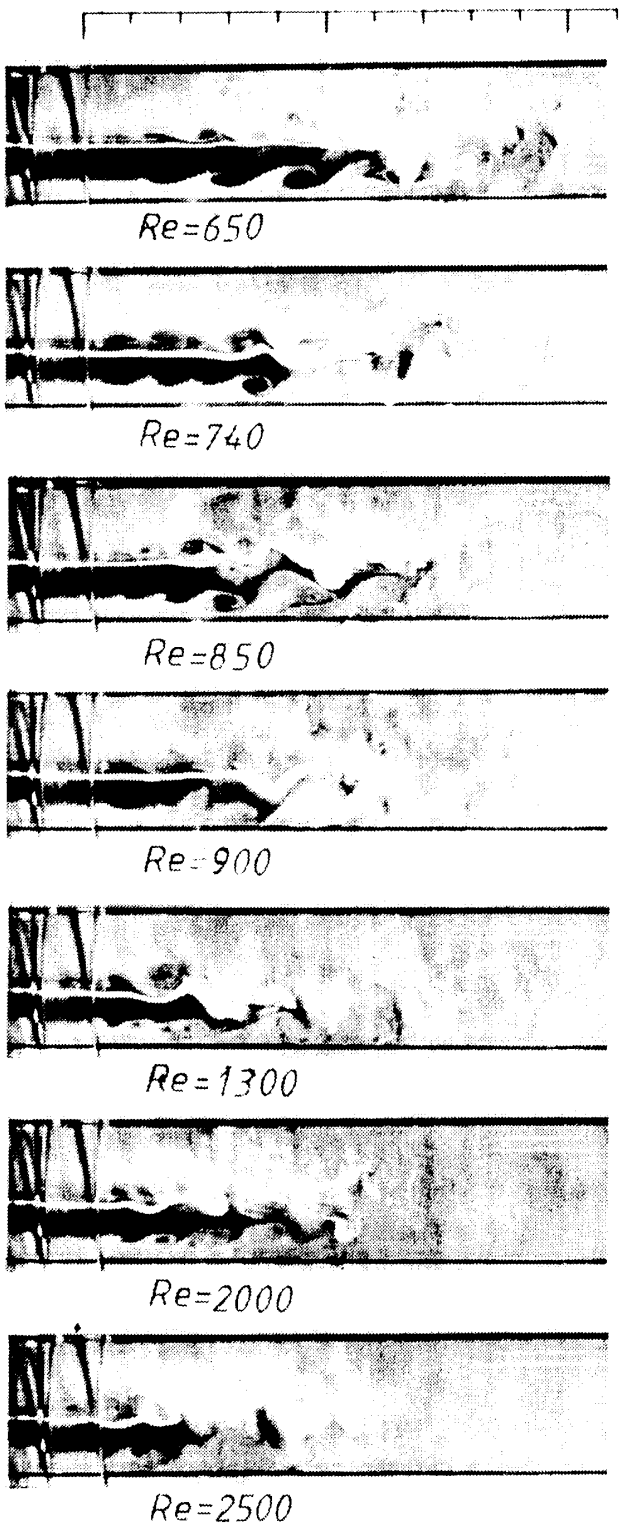

Fig. 9. Flow patterns by experimental observation.

This document is provided by JAXA.

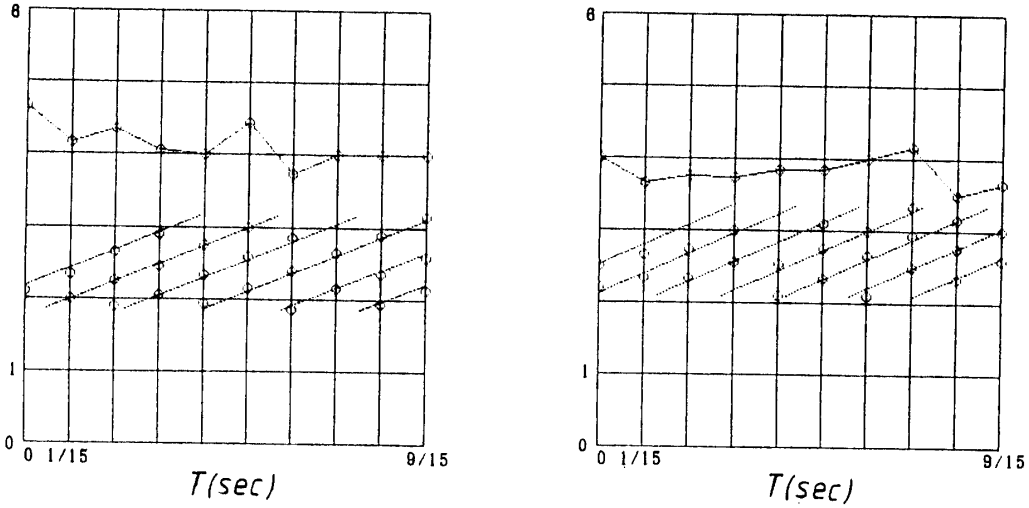

(a) at Re=570 (b) at Re=680

Fig. 10. History of vortices position by experimental observation.

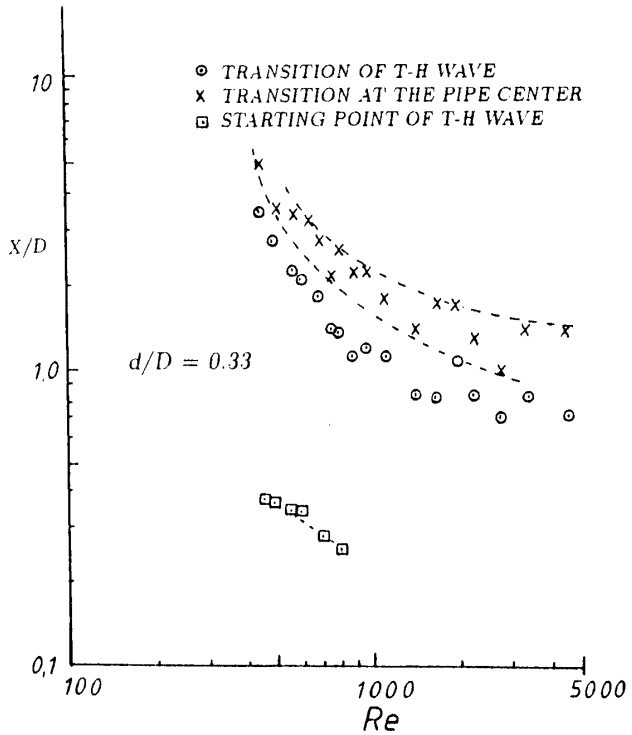

(a) d/D=0.33

Fig. 11. Experimental data of breakdown-transition.

This document is provided by JAXA.

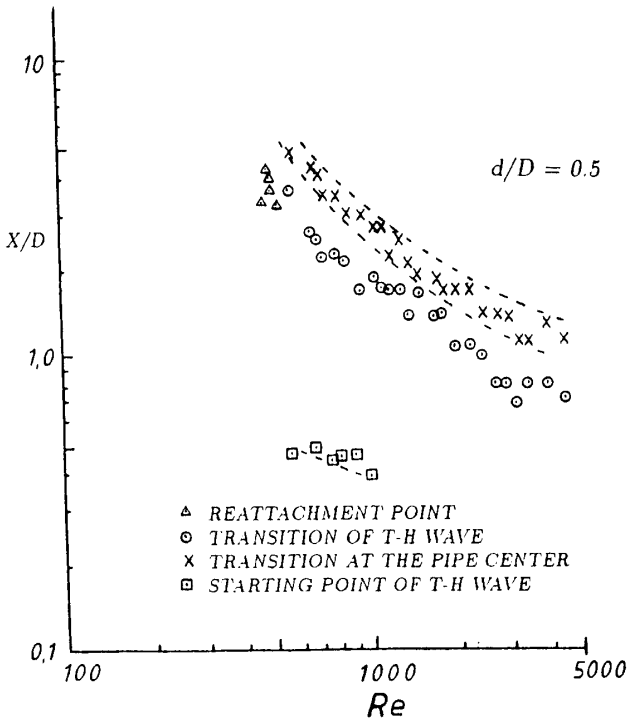

(b) d/D=0.5

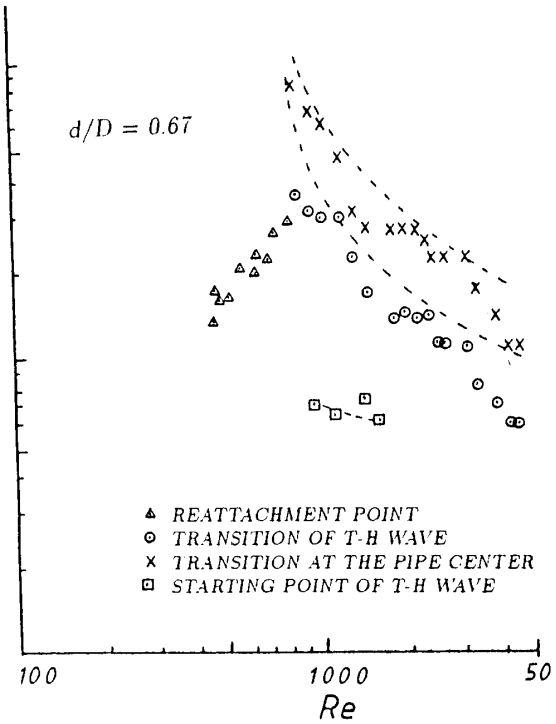

(c) d/D=0.67

Fig. 11 (Continued)

This document is provided by JAXA.

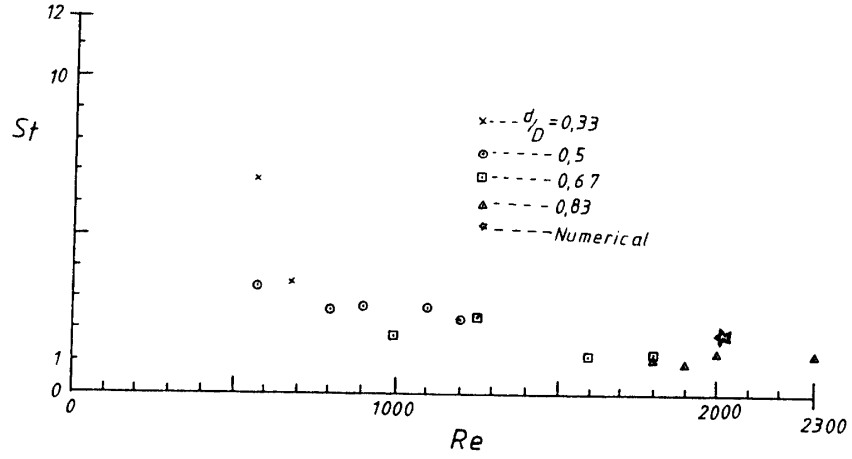

Fig. 12. Strouhal numbers of the turbulent blobs.

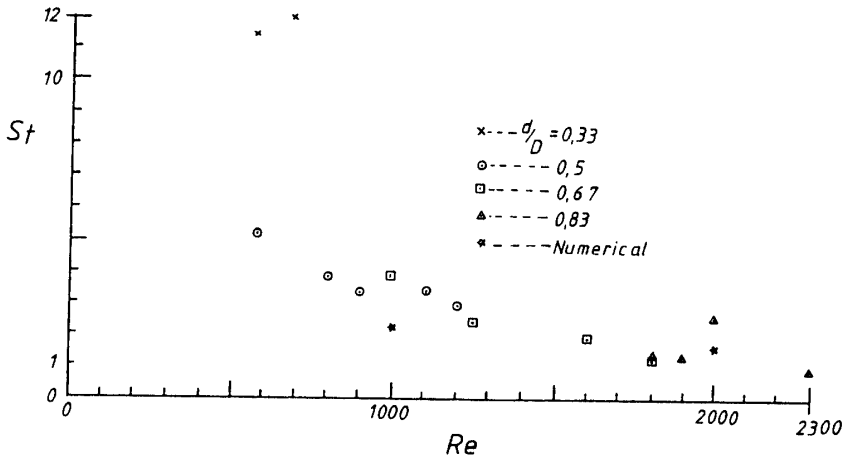

Fig. 13. Strouhal numbers of the T-H wave.

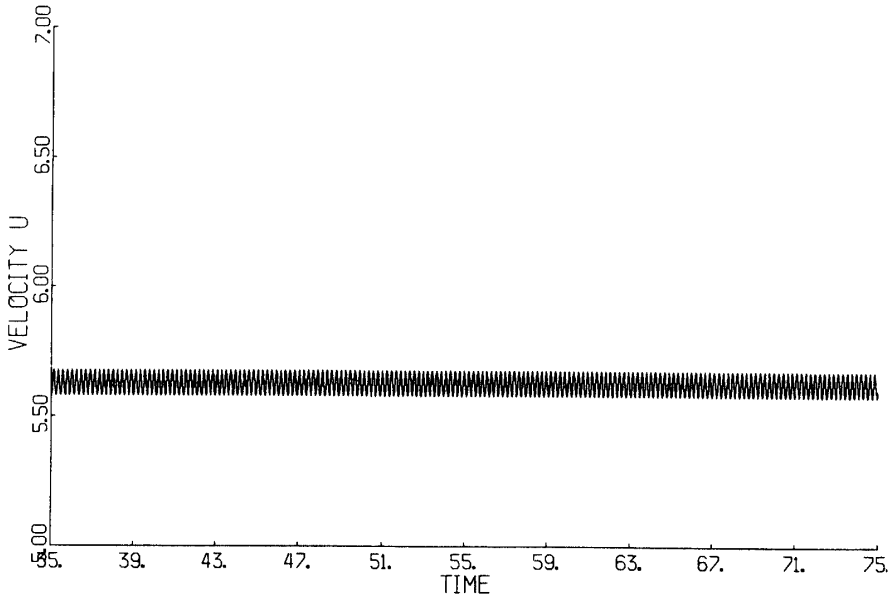

(a) at point 0.133L, 0.333R

Fig. 14. Velocity histry.

This document is provided by JAXA.

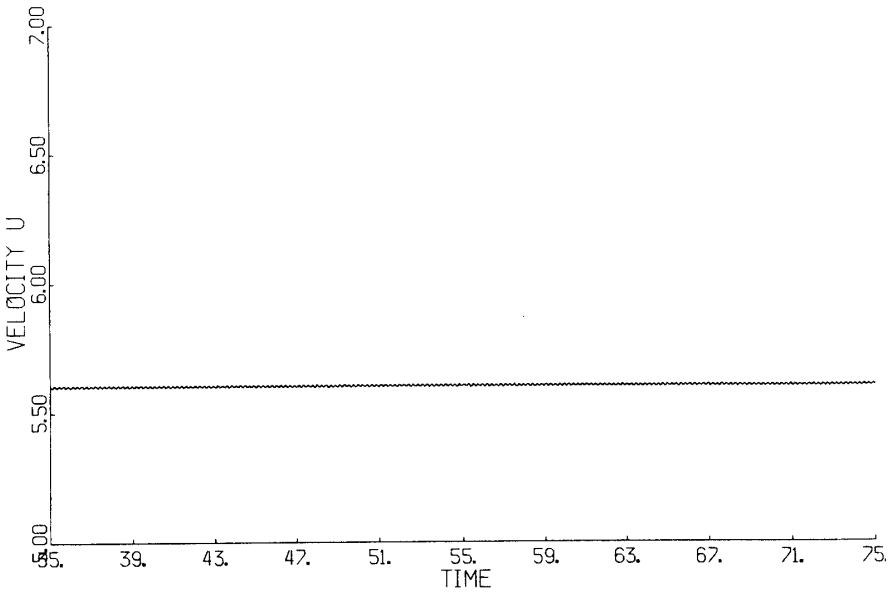

(b) at point 0.2L, 0.333R

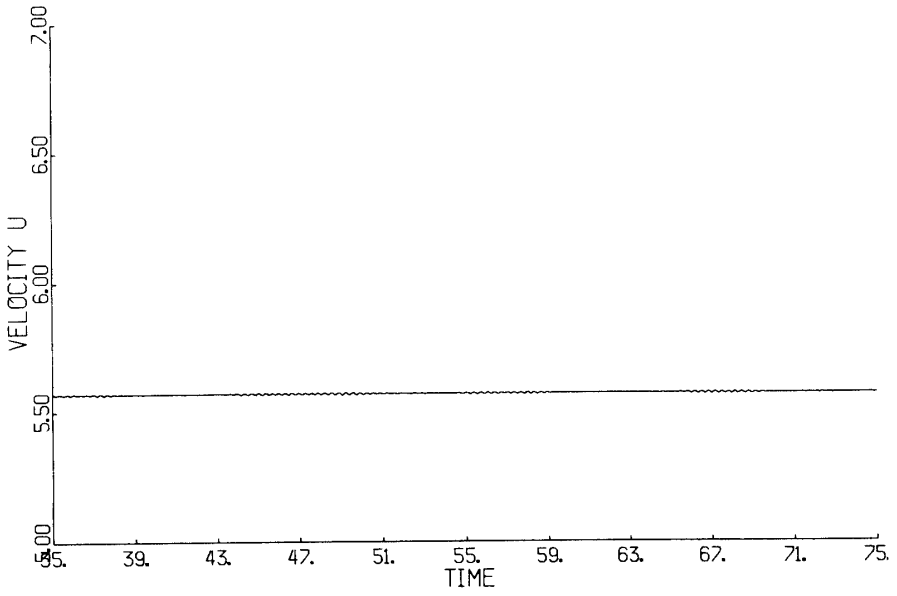

(c) at point 0.267L, 0.333R

Fig. 14 (Continued)

This document is provided by JAXA.

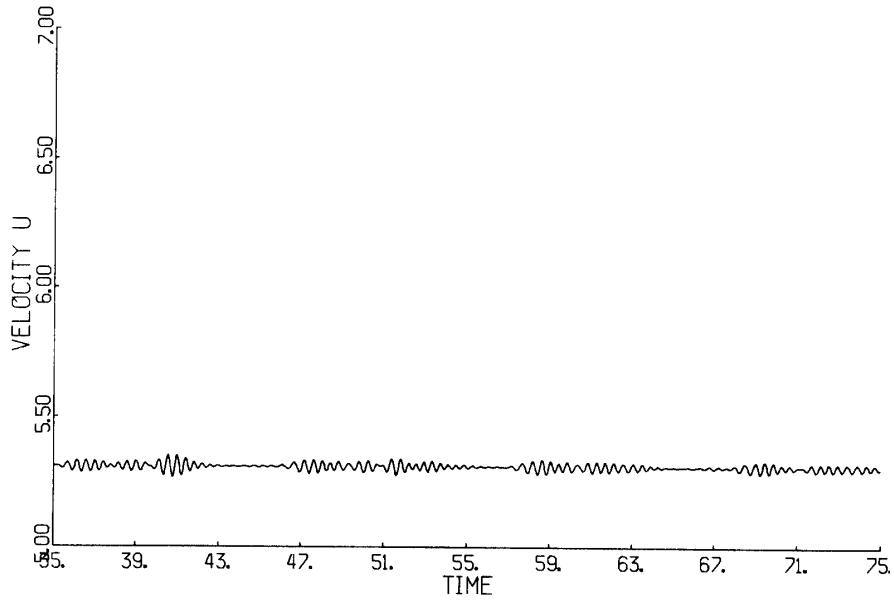

(d) at voint 0.733L, 0.333R

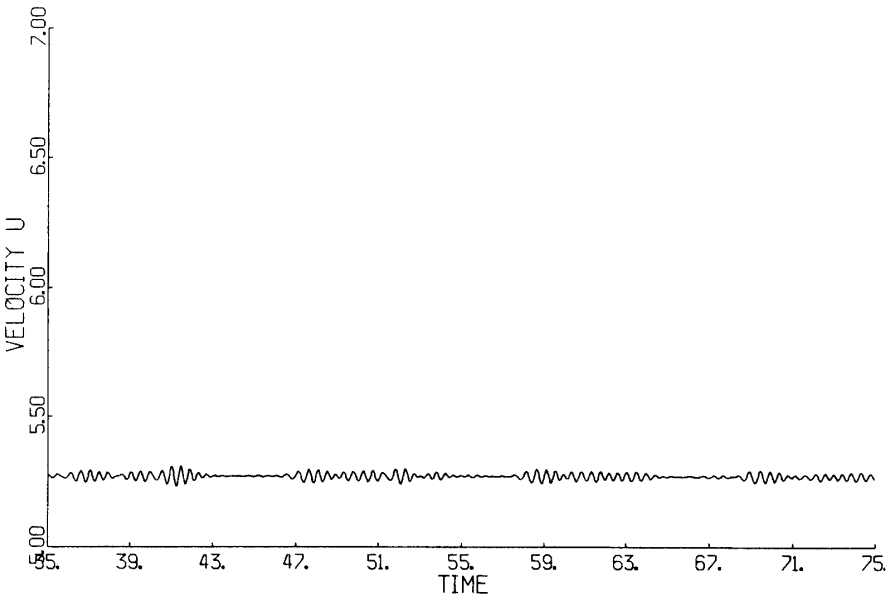

(e) at point 0.8L, 0.333R, the Reynolds number is 1000

Fig. 14 (Continued)

This document is provided by JAXA.

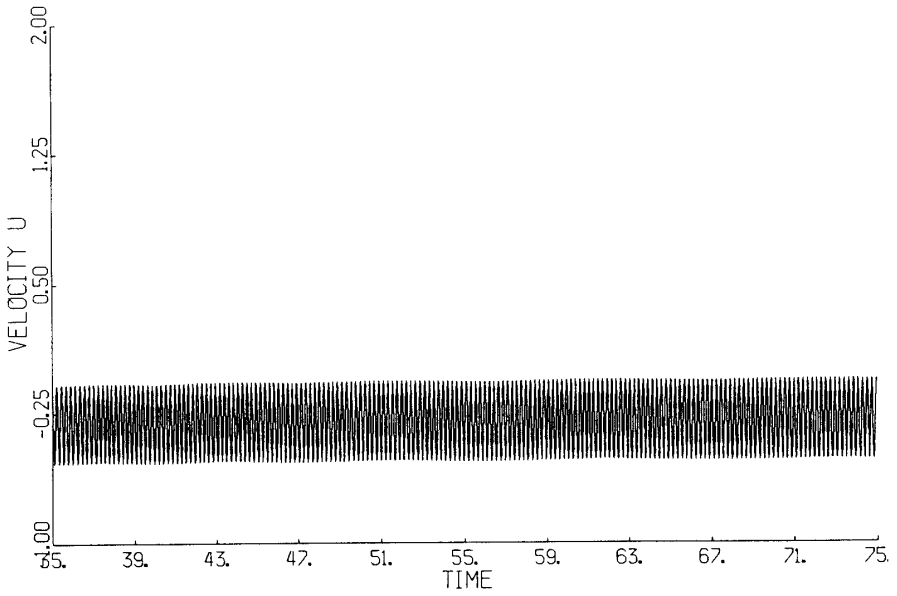

(a) at point 0.067L, 0.6R

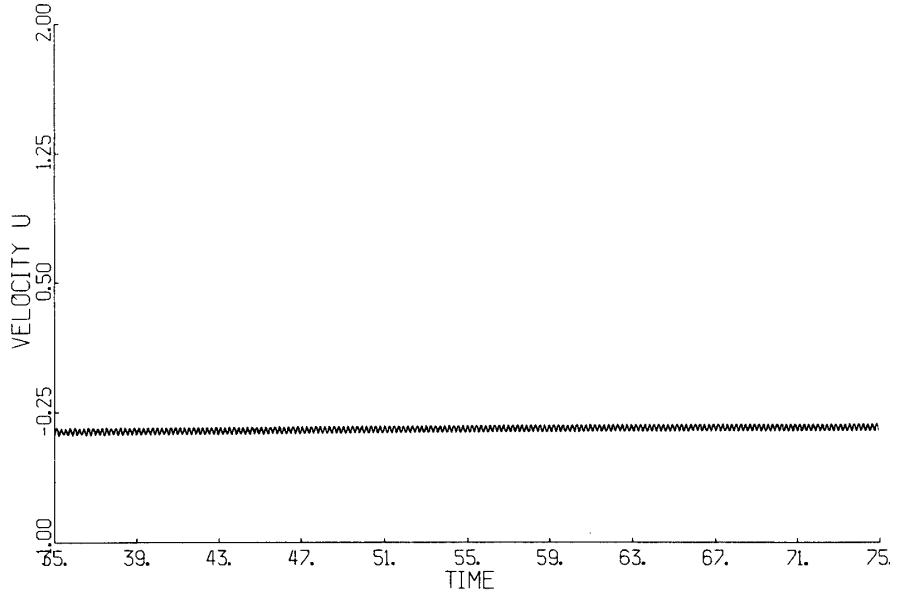

(b) at point 0.133L, 0.6R

Fig. 15. Velocity history.

This document is provided by JAXA.

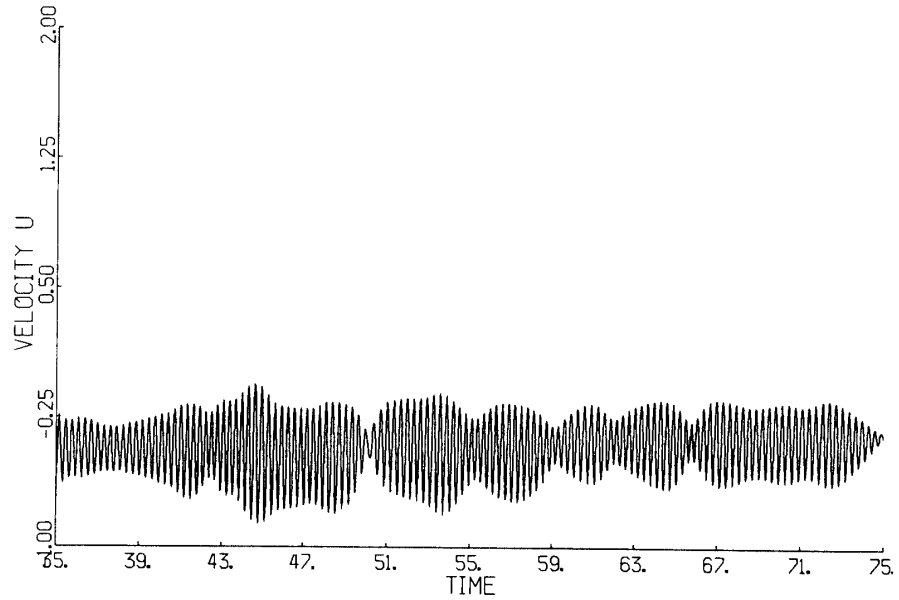

(c) at point 0.333L, 0.6R

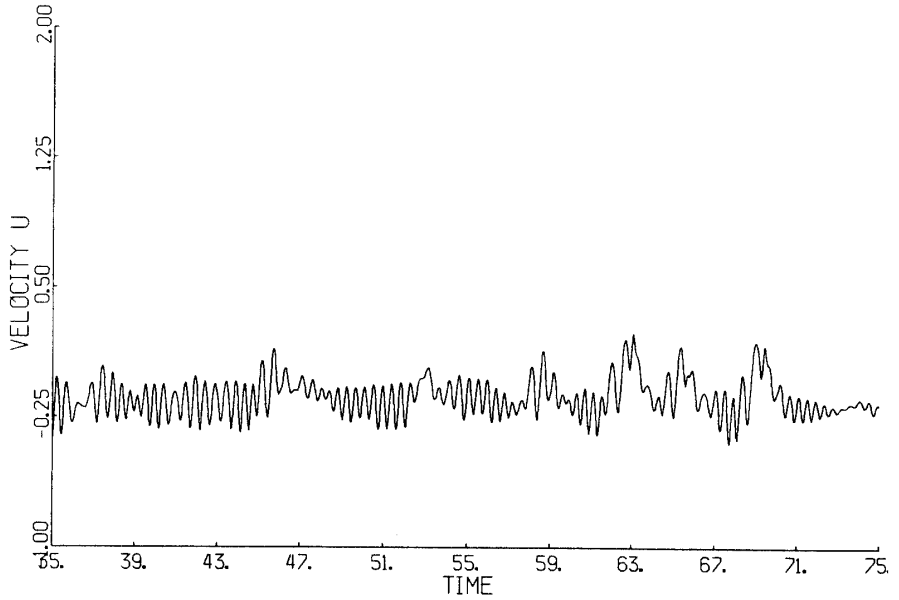

(d) at point 0.667R, 0.6R

Fig. 15 (Continued)

This document is provided by JAXA.

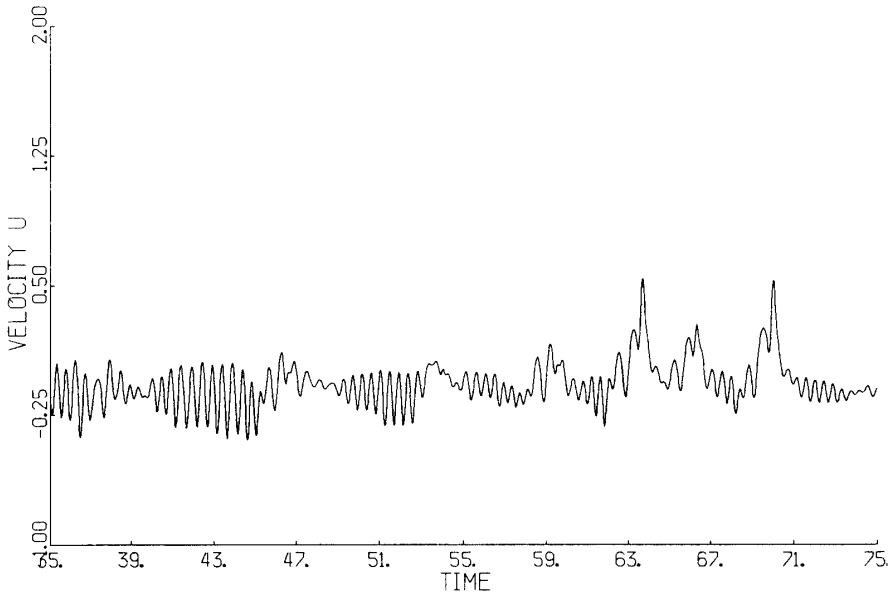

(e) at point 0.733L, 0.6R, the the Reynolds number is 2000

Fig. 15 (Continued)

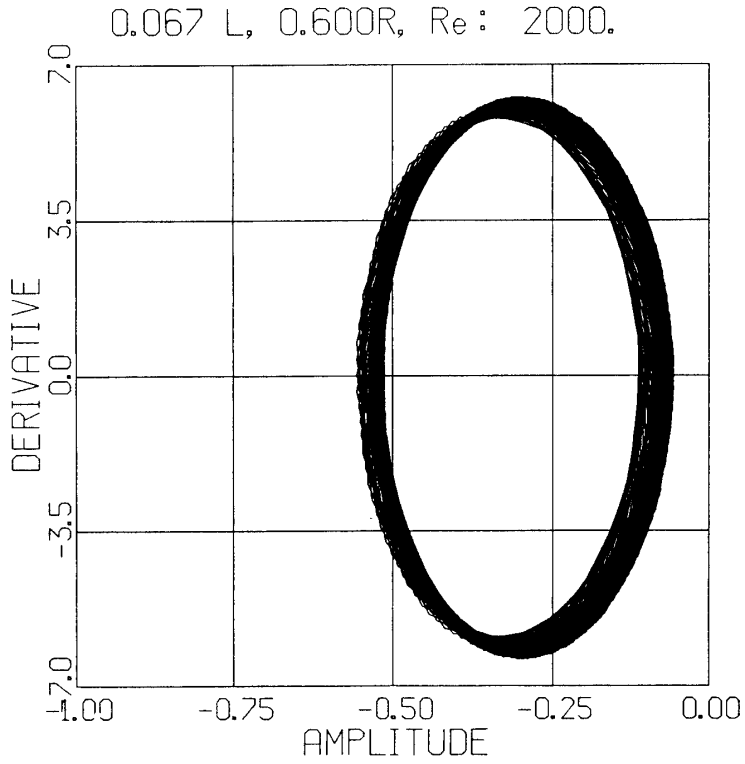

(a)

Fig. 16. Phase-space diagrams of velocity in the Fig. 15.

This document is provided by JAXA.

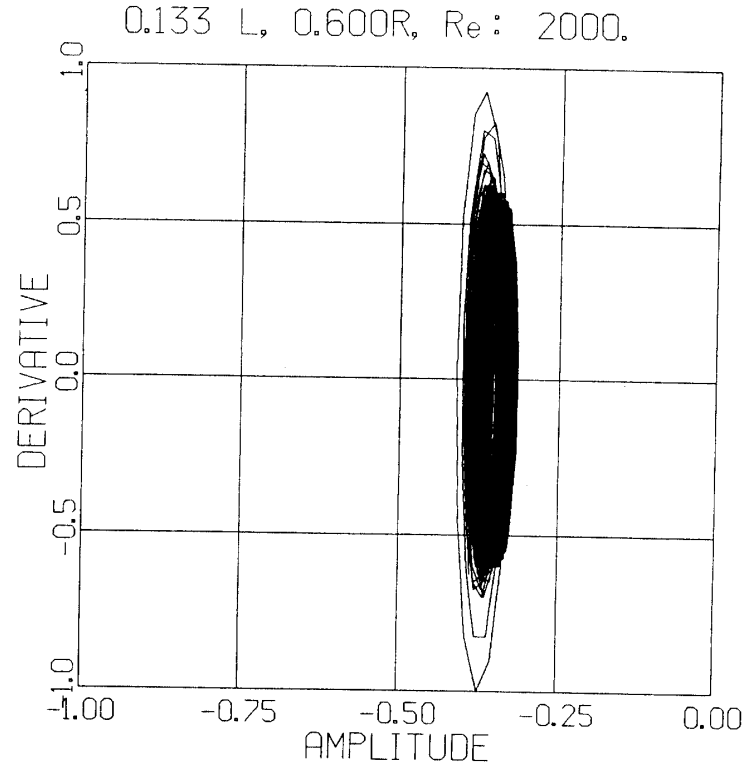

(b)

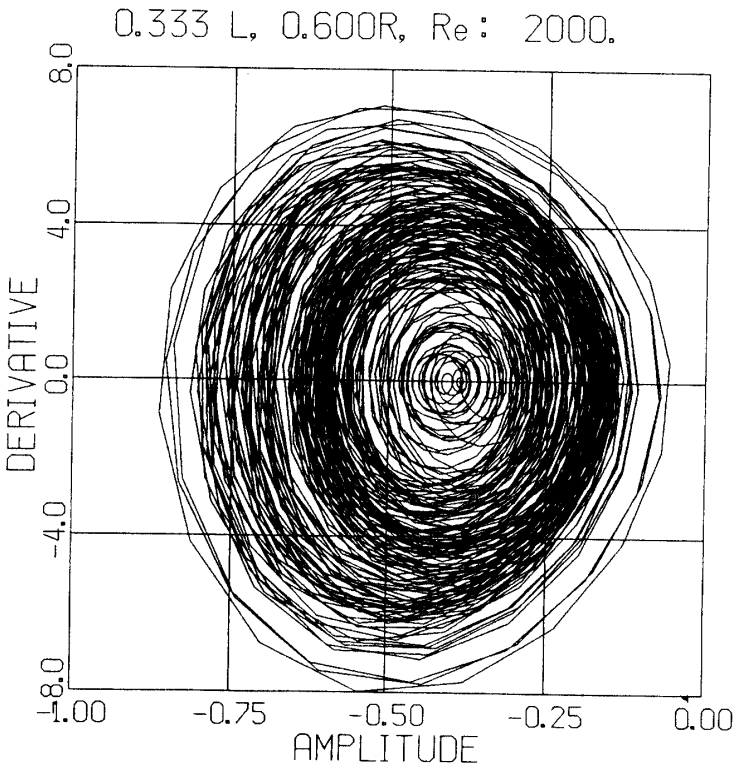

(c)

Fig. 16 (Continued)

This document is provided by JAXA.

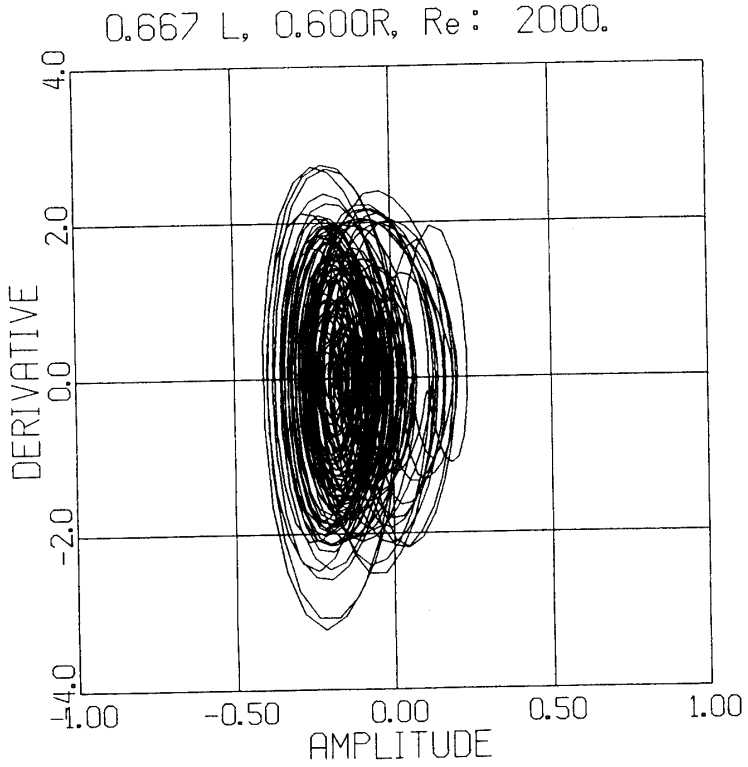

(d)

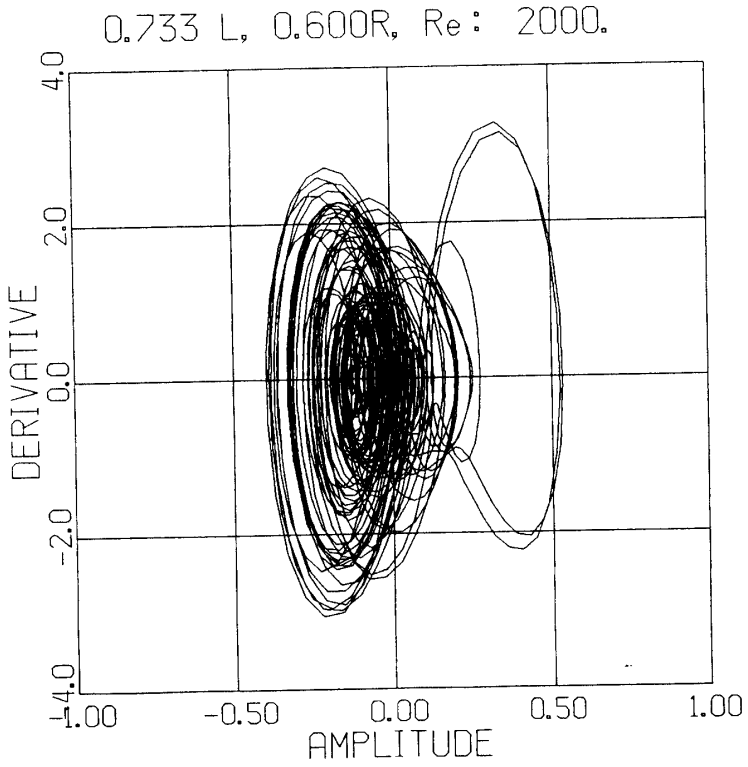

(e)

Fig. 16 (Continued)

This document is provided by JAXA.

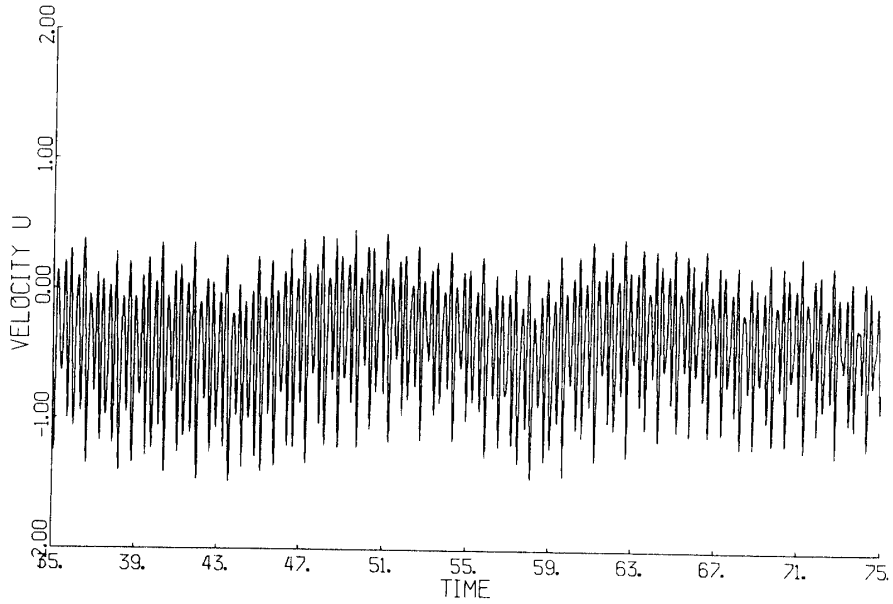

(a) at point 0.067L, 0.6R

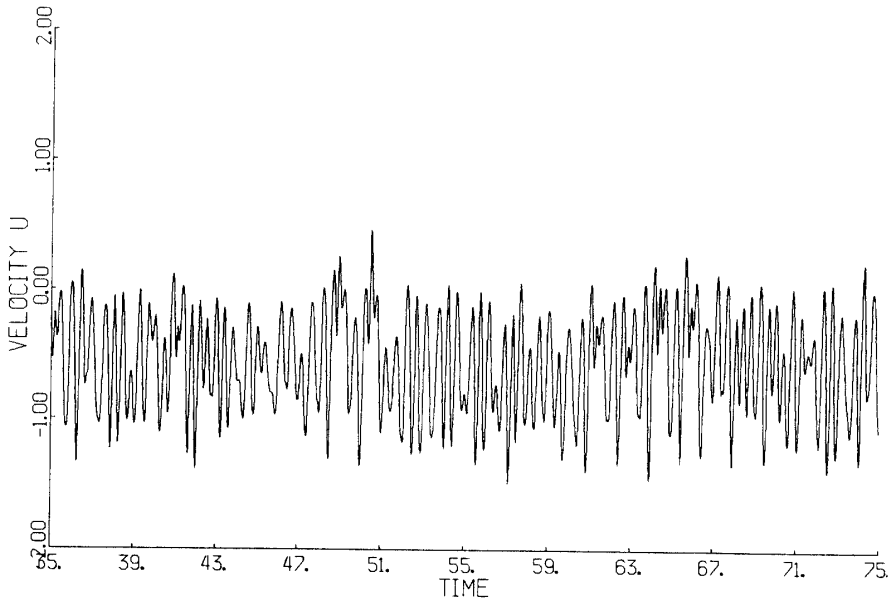

(b) at point 0.133L, 0.6R

Fig. 17. Velocity history.

This document is provided by JAXA.

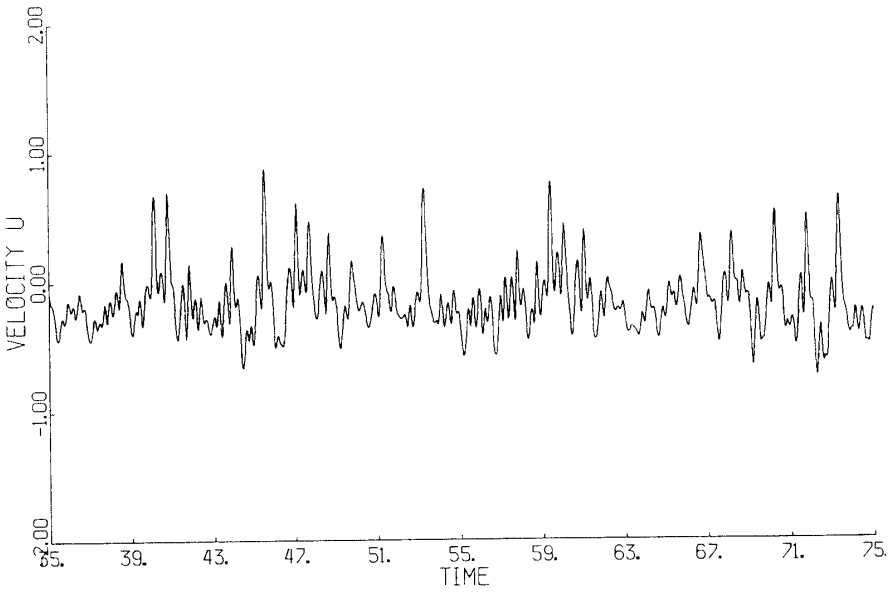

(c) at point 0.333L, 0.6R

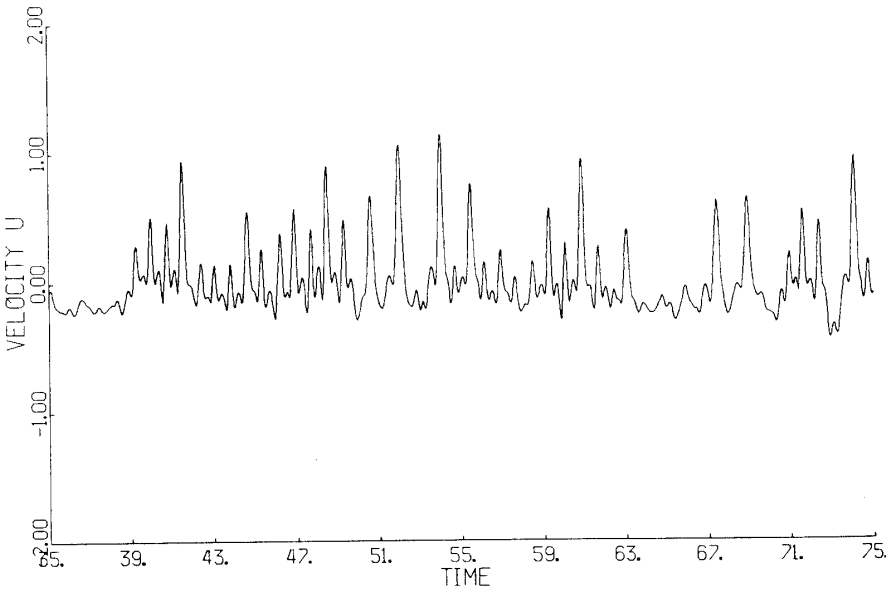

(d) at point 0.667L, 0.6R

Fig. 17 (Continued)

This document is provided by JAXA.

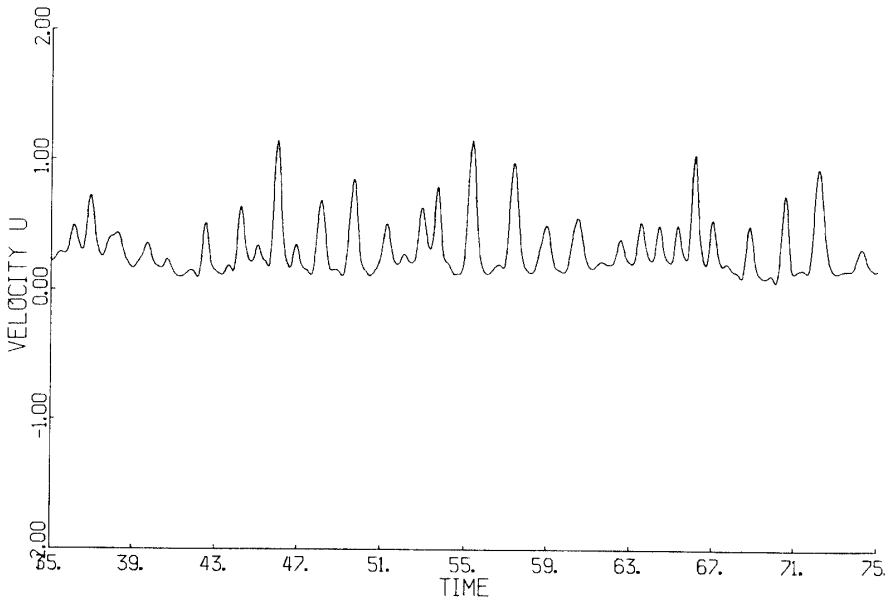

(e) at point 0.733L, 0.6R, the Reynolds number is 10000

Fig. 17 (Continued)

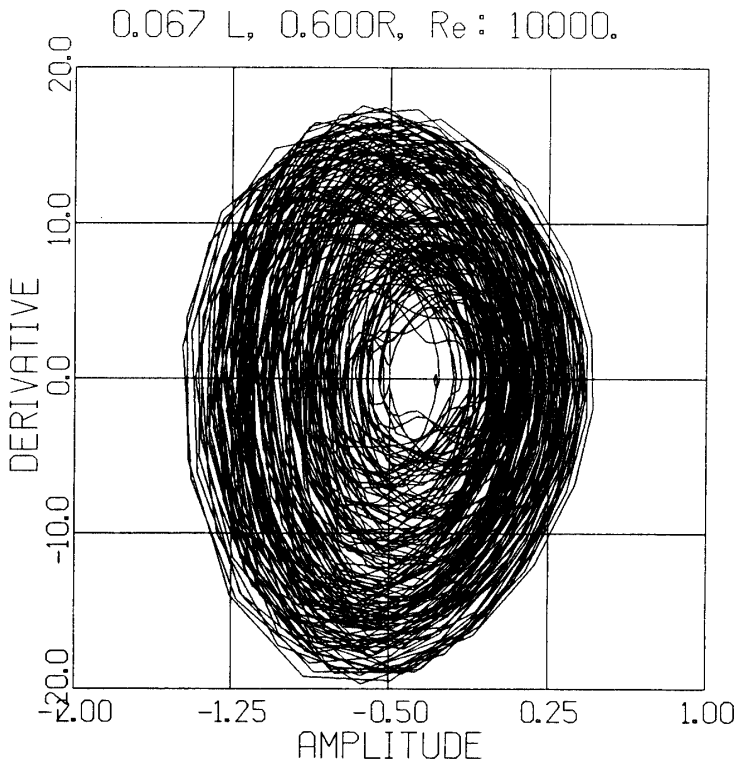

(a)

Fig. 18. Phase-space diagrams of velocity in the Fig. 17.

This document is provided by JAXA.

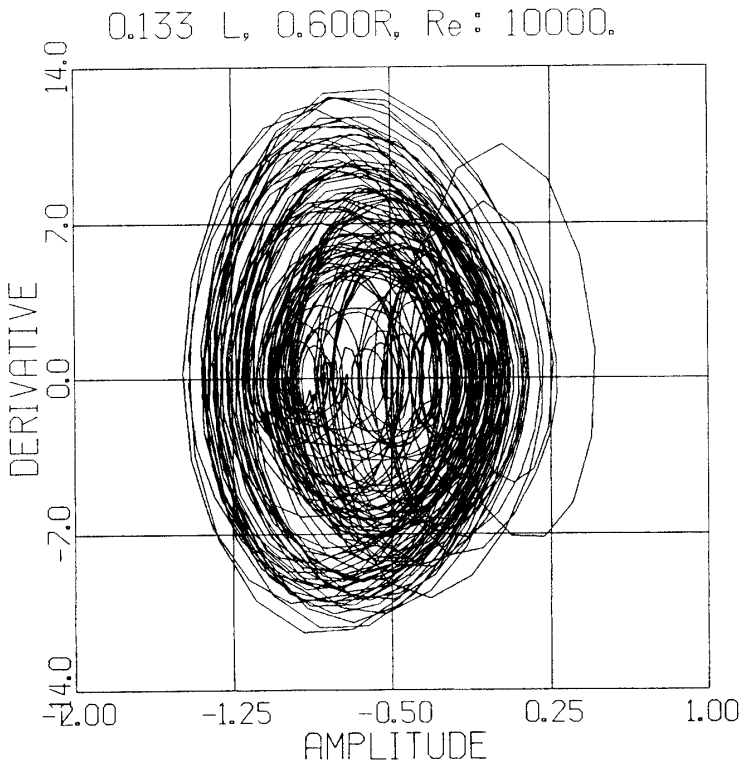

(b)

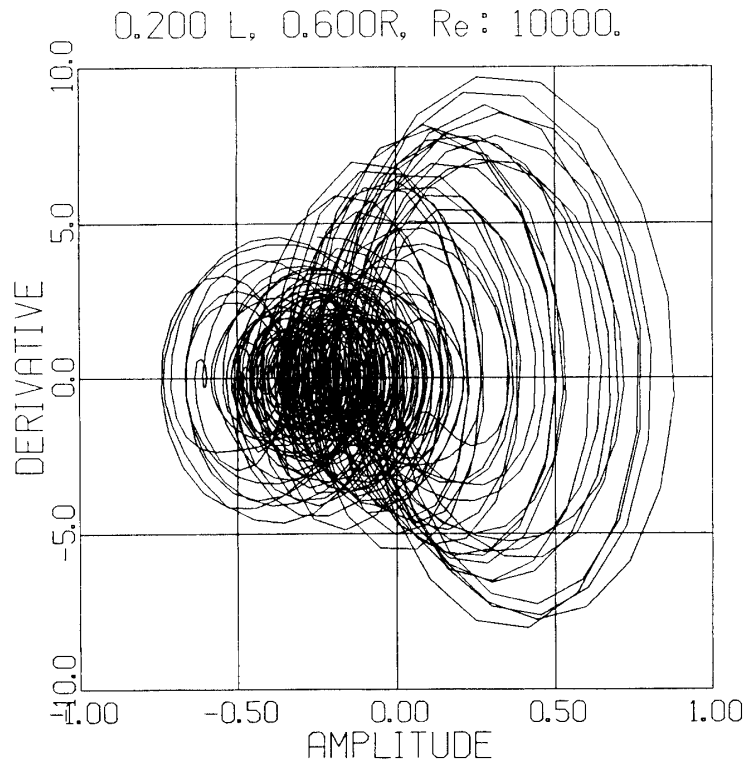

(c)

Fig. 18 (Continued)

This document is provided by JAXA.

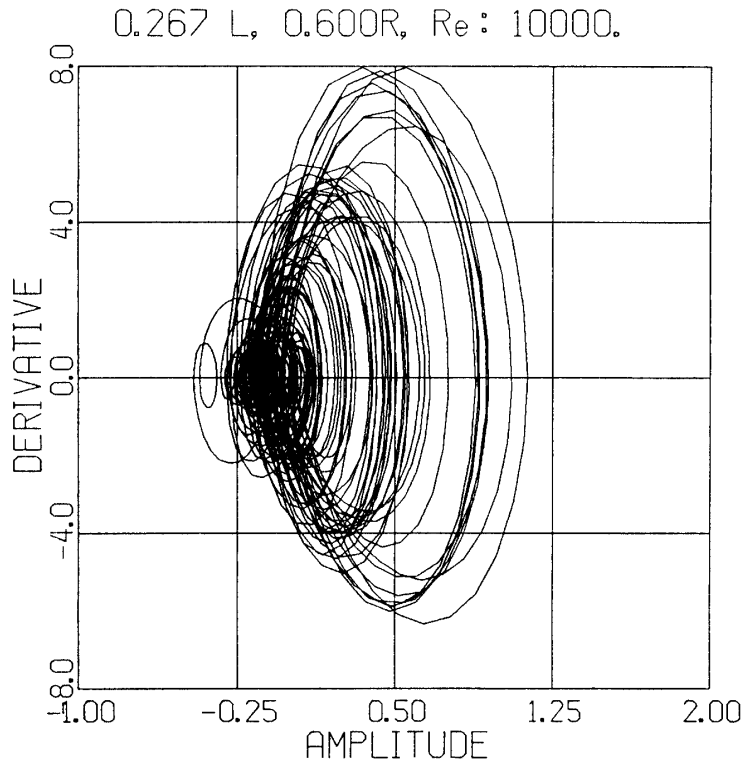

(d)

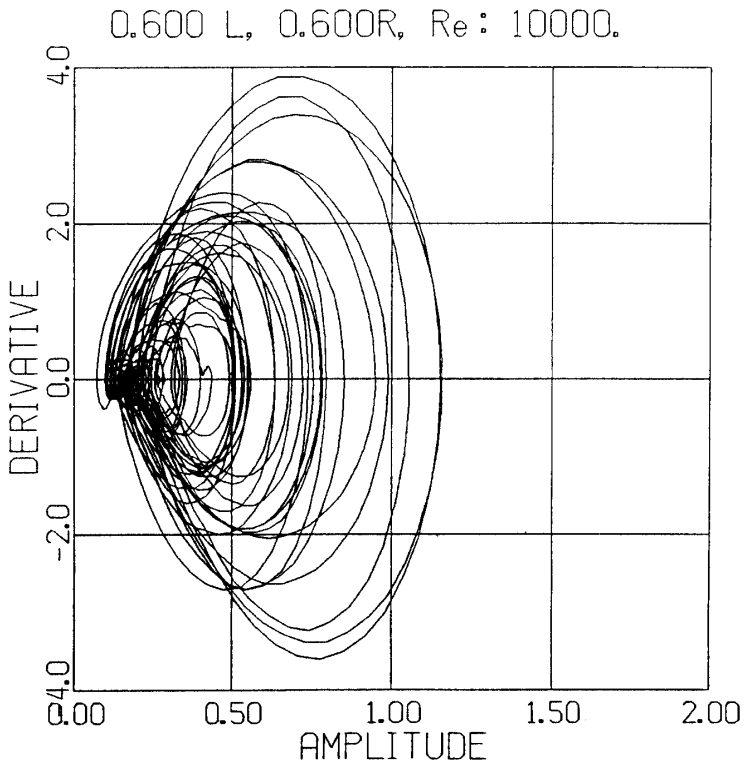

(e)

Fig. 18 (Continued)

This document is provided by JAXA.

certain Reynolds number and/or a swirling velocity, stagnation point appears on the symmetric axis and bubble-like breakdown of vortex takes place. The typical flow pattern are shown in Fig. 19. From numerical results, it is found that the presence vortex rings will early provoke the vortex breakdown, because the extension of stream tube between the two vortex rings causes the pressure increasing, then reverse flow appears on the axis, as shown Fig. 19. When sudden expansion gemetry is removed, flow instability is also different to that the swirling velocity is absent. Even under the axisymmetric assumption, when swirling velocity present and the Reynolds number excceds a certain value, the velocity dlistribution does not tend to Poiseuille type and reverse flow appears on the axis, after start from rest. That is, this type of flow is unstable.

3.2 Interaction of vortex rings and evolution into chaos

After Taylor-Helmholtz type instability cause the bursting of a street of vortex ring along the shear layer behind the sudden expansion, interaction of vortex rings plays dominant role in downstream. Typical case is shown in Fig. 7. Vortex rings a, b, c, d, e and f shed for a certain position continuously. Eventually, the a and the b, the e and the f merge into a large vortex ring, respectively. But no pairing take place between the c and the d. The position history of each vortex ring are plotted in Fig. 8. Timing and position of the vortex pairing is undefined. Caused by such complicated interaction of vortex rings, chaotic behavior appears in downstream. This is important because it

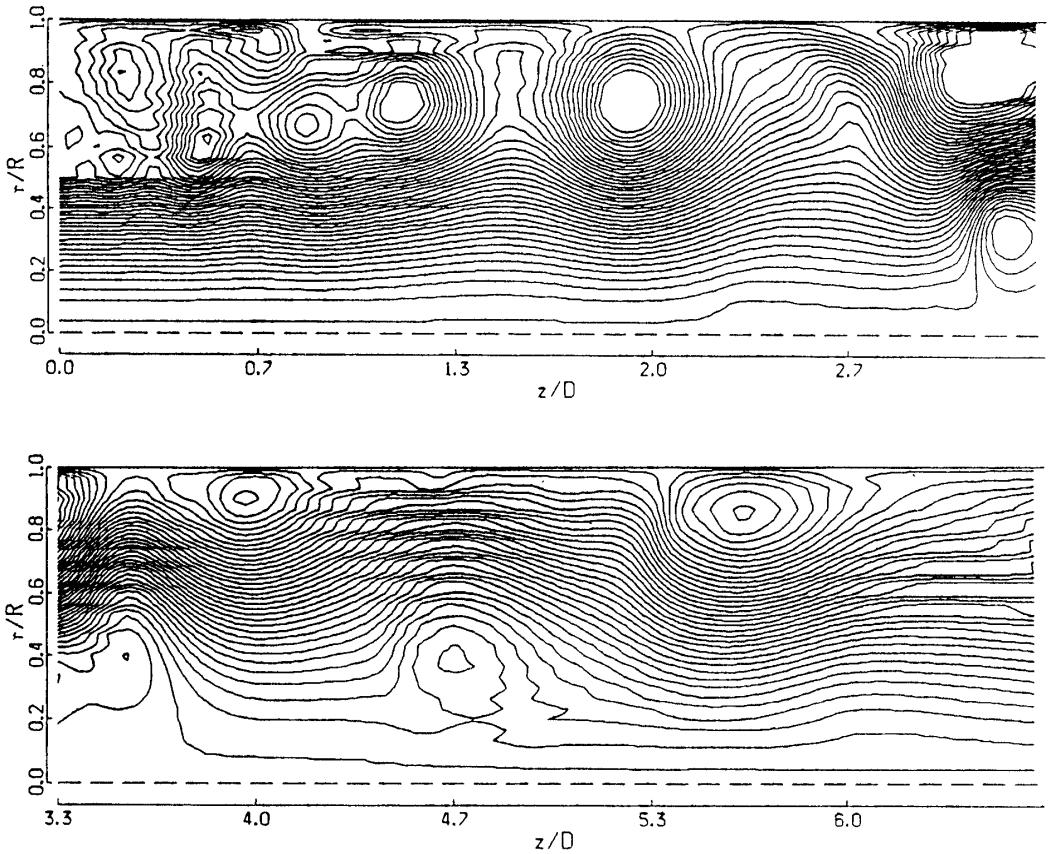

Fig. 19. Flow patterns after impulsively started from the rest condition with swiling velocity, the Reynolds number is 50000.

This document is provided by JAXA.

suggests the turbulence transition process.

Frequency characteristics of velocity at various Reynolds number were also investigated. At a low value 100 of the Reynolds number, no velocity oscillation appear behind the sudden expansion. As the Reynolds number increasing to 500, oscillation appears behind the sudden expansion but it dissipate immediately and flow tends to steady state. The numerical results reveals that the oscillation behind the sudden expansion is a simple periodic motion as long as over a certain Reynolds number,as shown in Fig. 14 (a), (b) and Fig. 15 (a), (b). As the Reynolds number increasing more, at 1000, the oscillation dissipate but not tend to steady flow. Intermittence wave appears in downstream, as shown in Fig. 14 (c), (d) and (e). At 2000 or higher value of Reynolds number, large variation take places in frequency characteristics at axis direction. Before the shedding point, the wave number do not change and simple periodic oscillation is kept. In the downstream, the merging of the vortex rings cause dissipation of high wave number oscillation, and the complicated interaction of vortex rings cause bifurcation from the simple periodic solution to chaotic one, as shown in Fig. 15 and Fig. 17.

Also important characteristics of the velocity, particularly the bifurcation of solution are obtained from phase-space diagrams. In the phase-space diagram, the horizontal axis is the velocity and the vertical axis is the derivative of the velocity. The phase-space diagrams of the velocity histories in Fig. 15 and Fig. 17 are plotted in Fig. 16 and Fig. 18, respectively. Chaotic behaviors and bifurcation processes of flow are recognized in these diagrams. Noted that the scaling is different at each diagram. In the downstream. Decreasing of the velocity amplitude by viscous dissipation can be seen.

4. Conclusion

It was experimental found that, for a certain range of the Reynolds numbers, a Taylor-Helmholtz type instability causes the shedding of a street of vortex rings along the shear layer bounding the stagnant region behind the step. This vortex street grows gradually and eventually occupies the whole pipe section. Bursting into a street of turbulent blobs occurs at this point. Numerical results successfully simulated detailed dynamical processes of vortex breakdown and growing into chaotic solutions. Numerical simulation reveals that vortical interaction of the vortex rings plays dominant role in this transition to turbulent blobs, which also confirmed by the physical observation. The Reynolds dependence of the Strouhal number of this turbulent blobs street was determined.

Acknowledgment

In this research, experimental work shown from Fig. 9 to Fig. 13 was carried out by Mr. Y. Ishii. The authors with to acknowledge his help.

This document is provided by JAXA.

Reference

[1] A. Fortin; A Numerical Simulation of the Transition to the Turbulence in a Two-Dimensional Flow, Journal of Computational Physics 70, 1987, pp311-329.

[2] J. Formm; A Numerical Study of Ekmen Boundary Layer Instability on Rotating Disk, Numerical Methods in Fluid Mechanics, edited by K. Oshima, 1986, vol.2, pp106-115.

[3] D.J.Latornell and A. Pollard; Some observations on the evolution of shear layer instabilities in laminar flow through axisymmetric sudden expansions, Phys. Fluid 29(9), 1986 pp2828-2835.

[4] K. Oshima, H.Kanda, Y.Ishii and H.L.Chen; Numerical Simulations of Unsteady Pipe Flows, Presented at the International Symposium on Computational Fluid Dynamics-Nagoya, August 28-31, 1989.

[5] H.Kanda, K.Oshima; Numerical Study of the Entrance Flows of a Circular Pipe, Proc. 10th ICNMFD, Lecture Note in Physics 264, ed. F.G.Zhuang, et al. pp363-368(1986).

[6] H.L.CHEN; Numerical Simulation of the Interaction of Vortex Rings in Viscous Fluid, Proceedings of the Symposium on Mechanics for Space Flight-1986. The Institute of Space and Astronautical Science, Report S.P.5, pp 15-22.

[7] H. Salwen and C.E.Grosch; The stability of Poiseuille Flow in a Pipe of Circular Cross-section, J.Fluid Mech. (1988), vol.190, pp375-392.

[8] John. Guckenheimer; Strange Attractor in Fluid: Another View, Ann. Rew. Fluid Mech. 1986. vol. 18. pp15-30.

[9] Marcel Escudier; Confined Vortices in Flow Machinery, Ann. Rew. Fluid Mech. 1987. vol. 19. pp 27-52.

[10] J.T.Stuart; Instability of flows and their transition to turbulence, ZFW Bd. 10 pp 379-392 (1986)

This document is provided by JAXA.